Endothelial cell flow-mediated quiescence is temporally regulated and utilizes the cell cycle inhibitor p27

Natalie T Tanke[a], Ziqing Liu[b], Michaelanthony T Gore[b], Pauline Bougaran[b], Mary B Linares[b], Allison Marvin[b], Arya Sharma[b], Morgan Oatley[b], Tianji Yu[b], Kaitlyn Quigley[b], Sarah Vest[b], Jeanette Gowen Cook[c], and Victoria L Bautch[a,b,d,#]

[a]Curriculum in Cell Biology and Physiology, The University of North Carolina at Chapel Hill, Chapel Hill, North Carolina 27599, USA
[b]Department of Biology, The University of North Carolina at Chapel Hill, Chapel Hill, North Carolina 27599, USA
[c]Department of Biochemistry and Biophysics, The University of North Carolina at Chapel Hill, Chapel Hill, North Carolina 27599, USA
[d]McAllister Heart Institute, The University of North Carolina at Chapel Hill, Chapel Hill, North Carolina 27599, USA

[#]Corresponding author: Victoria L Bautch, PhD
Professor of Biology
Department of Biology, CB#3280
University of North Carolina at Chapel Hill
Chapel Hill, NC 27599 USA
Email: bautch@med.unc.edu

Running head: Regulation of flow-induced endothelial quiescence depth

Words 7,195
Figures: 8
Supplemental Figures: 6
Supplemental Tables: 2 + Key Resources Table
References: 65
Abstract: 265 words

Keywords: Endothelial cell, laminar shear stress, quiescence depth, p27, cell cycle, zebrafish, *HES1*, *ID3*

ABSTRACT

Background: Endothelial cells regulate their cell cycle as blood vessels remodel and transition to quiescence downstream of blood flow-induced mechanotransduction. Laminar blood flow leads to quiescence, but how flow-mediated quiescence is established and maintained is poorly understood.

Methods: Primary human endothelial cells were exposed to laminar flow regimens and gene expression manipulations, and quiescence depth was analyzed via time to cell cycle re-entry after flow cessation. Mouse and zebrafish endothelial expression patterns were examined via scRNA seq analysis, and mutant or morphant fish lacking p27 were analyzed for endothelial cell cycle regulation and *in vivo* cellular behaviors.

Results: Arterial flow-exposed endothelial cells had a distinct transcriptome, and they first entered a deep quiescence, then transitioned to shallow quiescence under homeostatic maintenance conditions. In contrast, venous-flow exposed endothelial cells entered deep quiescence early that did not change with homeostasis. The cell cycle inhibitor p27 (*CDKN1B)* was required to establish endothelial flow-mediated quiescence, and expression levels positively correlated with quiescence depth. p27 loss *in vivo* led to endothelial cell cycle upregulation and ectopic sprouting, consistent with loss of quiescence. *HES1* and *ID3*, transcriptional repressors of p27 upregulated by arterial flow, were required for quiescence depth changes and the reduced p27 levels associated with shallow quiescence.

Conclusions: Endothelial cell flow-mediated quiescence has unique properties and temporal regulation of quiescence depth that depends on the flow stimulus. These findings are consistent with a model whereby flow-mediated endothelial cell quiescence depth is temporally regulated downstream of p27 transcriptional regulation by HES1 and ID3. The findings are important in understanding endothelial cell quiescence mis-regulation that leads to vascular dysfunction and disease.

GRAPHICAL ABSTRACT

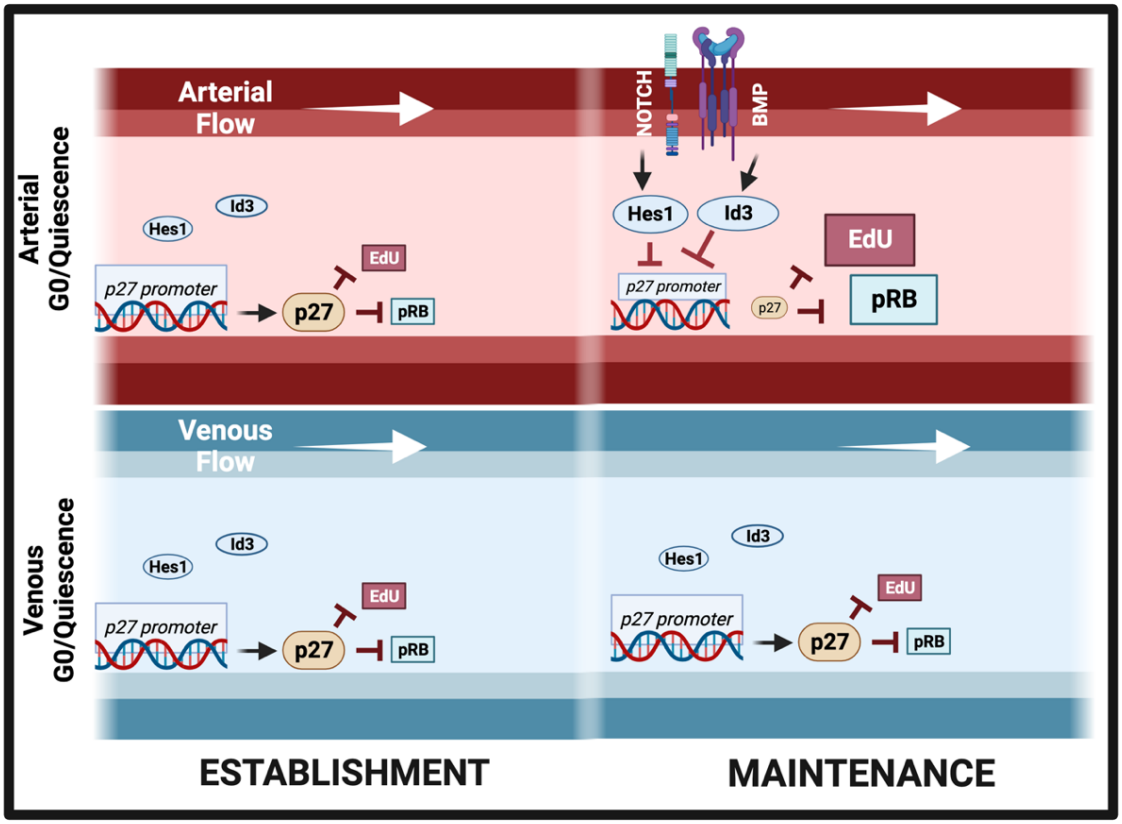

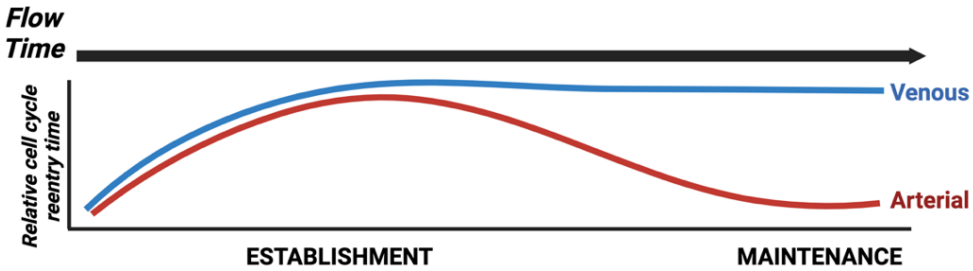

121 **HIGHLIGHTS**

122 - Different quiescence stimuli lead to distinct transcriptional and functional
123 quiescence profiles in endothelial cells
124 - p27 is required for endothelial cell quiescence and depth is temporally regulated
125 in a flow stimulus-dependent manner that correlates with p27 levels and flow-
126 regulated repressors *HES1* and *ID3*
127 - p27 is expressed in endothelial cells according to flow magnitude *in vivo* and is
128 functionally required for cell cycle regulation and sprouting *in vivo*

129 **INTRODUCTION**
130

131 Developmental blood vessel network expansion via sprouting angiogenesis leads
132 to remodeling and homeostasis; this transition depends on endothelial cell responses to
133 incoming signals, including laminar shear stress provided by blood flow. Laminar flow
134 leads to endothelial cell cytoskeletal realignment and dramatically reduces
135 proliferation[1–6]. Transcriptional profiles change with flow exposure[7,8], and signaling
136 pathways such as Notch and BMP are upregulated to promote alignment and vascular
137 homeostasis[9,10]. Vascular homeostasis significantly represses endothelial cell
138 proliferation and sets up a quiescent (G_0) state that can be released by angiogenic
139 growth factors such as VEGF-A[7,11,12]; [13–15]. How flow-mediated vascular quiescence is
140 established and maintained is poorly understood, yet it is critical to blood vessel
141 function.
142

143 Quiescence is influenced by cell type in non-endothelial cells[16,17], and
144 quiescence stimuli such as growth factor deprivation or contact inhibition also influence
145 quiescence parameters[18]. Different quiescence stimuli lead to transcriptional profiles
146 that are partially overlapping but have strong unique signatures[16,18]; however, how
147 these differences affect quiescence properties is poorly understood, and it is not known
148 how endothelial cells differentially respond to quiescence cues.
149

150 The cell cycle is regulated by cyclins and cyclin-dependent kinases (CDKs) that
151 promote and CDK inhibitors that block cell cycle progression[19]. In cycling cells, proteins
152 are post-translationally modified and/or carry destabilization sequences that lead to

153 rapid gain and loss of function required for passage through the cell cycle[20,21]. In
154 contrast, quiescence is characterized by transcriptional repression of cell cycle
155 activators and often by upregulation of cell cycle inhibitors[18,19]. Thus, cell cycle reentry
156 is delayed upon removal of the stimulus, and reentry time is used as a proxy for
157 quiescence depth[22,23]. Quiescence depth is variable; for example, quiescent fibroblasts
158 have delayed cell cycle reentry that positively correlates with temporal exposure to the
159 quiescence stimulus[22,23]. Non-homogeneous quiescence depth is associated with
160 muscle stem cells that respond to injury-induced circulating cues by entering a shallow
161 quiescence called "G_0 alert" that allows for prompt proliferation in response to a
162 subsequent injury[24]**.** Moreover, spontaneous quiescence was recently described,
163 whereby epithelial cells enter quiescence absent obvious environmental or
164 pharmacological cues, suggesting that quiescence entry has a stochastic component
165 and/or complex inputs[16,25]. Thus, how quiescence is established, maintained, and exited
166 is complex.
167
168 We examined properties of flow-induced endothelial cell quiescence and found
169 that arterial laminar flow-induced endothelial cell quiescence had a distinct
170 transcriptional profile and functionally exhibited dynamic temporal regulation of
171 quiescence depth, while venous flow did not exhibit the same temporal regulation of
172 quiescence depth. Temporal changes in endothelial cell quiescence depth positively
173 correlated with expression of the cell cycle inhibitor p27, and p27 repression and
174 temporal regulation of quiescence depth under arterial flow required *HES1* and *ID3*,
175 targets of the Notch and BMP signaling pathways. A requirement for p27 for endothelial

176 quiescence *in vivo* and correlation of p27 expression with flow magnitude was revealed.
177 Thus, flow-mediated endothelial cell quiescence is novel and complex, and regulation of
178 quiescence depth correlates with flow stimulus and likely influences physiological and
179 pathological vascular quiescence responses.
180
181
182 **MATERIALS AND METHODS**
183
184 ***Data availability***

185 Data associated with this study are available from the corresponding author upon
186 reasonable request. **Key Resources Table** is in Supplementary File.
187

188 ***Cell culture***

189 HUVEC and HAEC were cultured according to the manufacturer's
190 recommendations in EBM2 (Lonza#CC-3162) with growth factors (Lonza#CC-3162,
191 EGM2) at 37°C, 5% CO_2 and used between passages 2-4 (**Key Resources Table, cell**
192 **culture)**. Critical experiments were replicated with multiple lots of HUVEC and with
193 HAEC.
194

195 ***Microscopy***

196 Imaging was performed using confocal microscopy (Olympus Fluoview FV3000,
197 IX83) and a UPlanSApo 40x silicone-immersion objective (NA 1.25), UPlanSApo 60x
198 oil-immersion objective (NA 1.40), or UPlanSApo 100x oil-immersion objective (NA
199 1.40). Images were acquired with Fluoview FV31S-SW software and imaging analysis

200 was completed in FIJI[26]. For each replicate within an experiment, images were acquired
201 at the same settings.
202
203 ***Endothelial Cell Transfection***
204 HUVEC were grown to sub-confluency and treated with siRNAs **(Key Resources**
205 **Table, siRNA information)** diluted in OptiMem (Gibco, #11058021) and Lipofectamine
206 3000 (ThermoFisher, #L3000015) according to manufacturer's protocol
207 (https://www.thermofisher.com/us/en/home/references/protocols/cell-
208 culture/transfection-protocol/lipofectamine-2000.html). Briefly, siRNA at 0.48 μM in Opti-
209 MEM (31985-070, Gibco) and a 1:20 dilution of Lipofectamine in Opti-MEM were
210 incubated separately at RT for 5 min, then combined and incubated at RT for 15 min.
211 HUVEC were transfected at 80% confluency with siRNA at 37°C for 24h, then in 10 mL
212 of fresh EGM-2. All experiments were initiated 48h following siRNA exposure.
213
214 ***Immunofluorescence and EdU labeling***
215 Endothelial cells were fixed in 4% PFA (15713 (100504-940), VWR) at 37°C for
216 10 min, permeabilized in 0.1% Triton (T8787-100ML, Sigma) in PBS for 10 min at RT,
217 then blocked for 1h at RT in 5% NBCS (Gibco, #16010-159), antibiotic-antimycotic
218 (Gibco, #15240062), 0.1% sodium azide (Sigma s2002-100G). Following 3X PBS
219 washes, cells were incubated in primary antibody/blocking solution and incubated for
220 24h at 4°C (**Key Resources Table, antibodies**), washed 3X with PBS and incubated in
221 secondary antibody/blocking solution for 3h at RT in the dark (**Key Resources Table,**
222 **antibodies**). Slides were mounted with coverslips using Prolong Diamond Antifade

223 mounting media (P36961, Life Technology), sealed with nail polish, and stored at 4°C.
224 Glass-bottom Ibidi slides or well dishes were stored in 1X PBS. For all nuclear stains,
225 The DAPI channel was used as a nuclear mask, and nuclear fluorescence intensity was
226 measured for each cell per image field. Positive cells were defined as those above the
227 sensitivity threshold.
228
229 EdU labeling was performed according to the Click-IT EdU 488, 594, or 647
230 protocol (Invitrogen, C10337). Cells were incubated in EdU for 30 min (quiescence
231 depth) or 1h at 37°C in 5% CO_2 and fixed with 4% PFA for 10 min at RT.
232
233 ***Quiescence Depth***
234 Flow: HUVEC were cultured in EBM2 supplemented with 2% FBS, 1% antibiotic-
235 antimycotic (Gibco, #15240062), and 1% Nystatin (Sigma, #N1638-20ML) and exposed
236 to laminar flow for indicated times and shear levels using an Ibidi pump system (CC-
237 1090, Ibidi). Static (non-flow) control slides were seeded at lower densities and
238 incubated for 48h prior to fixation with 4% PFA. For western blot experiments, an orbital
239 shaker (Hoefer Red Rotor Mixer Platform Shaker PR70-115V) was used as previously
240 described[27]. Flow-mediated quiescence depth experiments were performed after 16h or
241 72h of laminar flow exposure by incubation for 30 min with EdU, fixation at indicated
242 times post-flow in 4% PFA for 10 min at RT, then visualized for EdU and/or stained for
243 antibodies as described **(Supp. Tables S2, S3)**.
244

245 Contact: HUVEC were seeded in a 6-well plate at 1.2 X 10^6 cells/well (high
246 density) or 0.2 X 10^6 cells/well (low density) and incubated for 24h. A p1000 pipette tip
247 was used to scrape the cell monolayer and create a gap, as previously described[28],
248 cells were incubated with EdU for 30 min or fixed at 0h, 2h, 5h, or 8h post-scratching in
249 4% PFA for 10 min at RT, then visualized for EdU and/or stained for antibodies as
250 described **(Supp. Table S2, S3)**. Cells within 1000μm of the scratch edge were imaged
251 **(Supp. Fig. 2a)**.
252
253 ***Cell Axis Ratio***
254 Cell shape and alignment were measured as described previously[7]. Cells were
255 stained for VE-cadherin upon fixation, and measured at the longest axis of cell divided
256 by shortest axis to calculate the cell axis ratio, with the longest cell axis being the
257 direction of flow.
258
259 ***Western Blot Analysis***
260 Western blot analysis was performed according to[29] with modifications. Briefly,
261 cells were scraped into PBS, centrifuged at 13000 rpm (4°C, 20 min), resuspended in
262 RIPA buffer with protease/phosphatase inhibitor (5872S, Cell Signaling), then added to
263 sample loading buffer with dithiothreitol (R0861, Thermo Fisher) and boiled for 10 min.
264 Samples (10ug) were separated on 10% SDS-PAGE gel (161-0183, BioRad), then
265 transferred to a membrane, incubated in primary antibodies (overnight, 4°C) (**Key
266 Resources Table, antibodies**), washed 3X in PBST and stained with secondary
267 antibody in One-Block (RT, 1h) (**Key Resources Table, antibodies**). Immobilon Forte

268 HRP Substrate (WBLUF0100, 769 Millipore Sigma) was added for 30 sec, and blots
269 were exposed for 2 sec ChemiDoc XRS with Chemi High Resolution setting.
270
271 ***RNA***
272 RT-qPCR: Scraped cell pellets were resuspended in TRIzol (15596018,
273 Invitrogen). cDNA was generated from 1ug RNA using iScript reverse transcription kit
274 (Bio-Rad, #1708891) and diluted 1:3 in water. qRT–PCR was performed using iTaq
275 Universal SYBR Green SuperMix (Bio-Rad, #1725121). SYBR Green real-time PCR
276 was performed in triplicate on the Applied Biosystems QuantStudio 6 Flex Real-Time
277 PCR System (**Key Resources Table, qPCR primers**). For quantification, relative
278 expression of each gene to β-actin in each sample was calculated by 2^ (CT of
279 gene−CT of β-actin). Statistical significance was determined by unpaired Student's T-
280 test.
281
282 Bulk RNA seq: 3 Ibidi slides/condition were pooled, and stranded libraries were
283 prepared using KAPA mRNA HyperPrep Kit (7961901001, Roche) and sequenced
284 using NovaSeq S1 at the UNC Sequencing Core. Data was analyzed as described
285 previously [30]. Briefly, 2–3×10^7 50 bp paired-end reads per sample were obtained and
286 mapped to the human genome GRCh38 with STAR using default settings[31]. Quality of
287 sequencing reads was confirmed with FastQC before mapping. Mapping rate was over
288 87% for all samples **(Supp. Table S2)**, and gene (GEO GSE213323) expression was
289 determined with Htseq-count using the union mode[32] . Genes with low expression were
290 filtered out (total raw counts in all samples <10), differential expression analysis was

291 performed with DESeq2 [33] using default settings in R, and lists of differentially
292 expressed genes were obtained (p adjusted <0.1). Gene ontology analysis was
293 performed using enrichGO function in the R package clusterProfiler. All gene ontology
294 terms shown in this study have a corrected P value <0.1.
295
296 Mouse scRNAseq: A mouse scRNAseq dataset (Liu et al, in preparation) (GEO
297 GSE216594) previously generated using enriched endothelial cells from the mouse ear
298 at P8 (postnatal day 8) was analyzed for *Cdkn1b* levels in endothelial cells.
299
300 ***Quiescence Score***
301 The endothelial quiescence score was calculated using the formula: QS =
302 1/n$\sum_{i=1}^{n} QSUi$-1/m$\sum_{j=1}^{m} QSDj$ (QS = Quiescence Score, QSU = QS of upregulated genes
303 under quiescence (total n genes), QSD = QS of downregulated genes under quiescence
304 (total m genes)). Selected genes were upregulated or downregulated relative to static
305 samples. All genes were normalized for sequencing depth and scaled for expression as
306 previously described[8]. To generate the gene list used for endothelial quiescence score
307 we utilized two datasets **(Supp. Table S1)**: S/G_2/M phase associated genes from the
308 CellCycleScoring function of the R package Seurat that were down-regulated with flow
309 in scRNAseq HUVEC (accession code GSE151867)[8], and genes that were upregulated
310 with different quiescence stimuli in non-endothelial cells[18] and upregulated with flow in
311 scRNAseq data. The epithelial quiescence score was developed by the Barr lab as
312 previously described, and utilized an independent gene list generated using non-
313 transformed human epithelial cell data[16,34].

314 ***Zebrafish***

315 Zebrafish (*Danio rerio*) were housed in an IACUC approved facility[30].
316 *Tg(fli:LifeAct-GFP*) was a gift from Dr. Wiebke Herzog **(Key Resources Table,**
317 **animals)**. The *cdkn1bb* CRISPR line was designed as previously described **(Key**
318 **Resources Table**, **genetically modified animals)**[35]. One-cell stage zebrafish embryos
319 were injected with 1nl injection solution into the cytoplasm. Fin clips were used to
320 identify possible founders with gene-flanking primers PCR (F-
321 CTCAATAACTGCTGCGAGTG, R- GATGAAGGGGGGAAAGAGG, R-
322 GCCATCGAGTCAAACCAG).
323
324 Morphant fish were obtained by randomly injecting 2.5–5 ng of non-targeting
325 (NT) (5'-CCTCTTACCTCAGTTACAATTTATA-3', GeneTools, LLC) or *cdkn1bb* (5'-
326 ACGGTCAAAATTCAAAGCACATACC 3', GeneTools, LLC) MO into *Tg(fli:LifeAct-GFP*)
327 embryos at the one-cell stage. Fish were grown in E3 medium at 28.5°C to 36hpf.
328
329 Embryos were prepared for imaging as previously described[30]. Briefly,
330 dechorionated embryos were fixed overnight in ice-cold 4% PFA at 4 ºC, rinsed 2X in
331 PBS, mounted using Prolong Diamond Antifade mounting medium (P36961, Life
332 Technology), and coverslip sealed with petroleum jelly.
333
334

335 ***Zebrafish FACs Sorting***

336 FACs sorting was as previously described[36]. Briefly, embryos were euthanized in
337 1X Tricaine, dissociated with 100mg/mL collagenase in 1X PBS and 0.25% trypsin and
338 harsh mechanical pipetting, and incubated (30ºC, 10 min). The dissociation reaction
339 was neutralized with DMEM + 10% FBS and cells were centrifuged (5000 rcf, 5 min).
340 Pellets were resuspended in 500μL DMEM/FBS and filtered using a 30μm cell strainer.
341 Samples were analyzed on the AttuneX (UNC Flow Cytometry Core), and GFP+ cells
342 from *fli:LifeAct-GFP* embryos were collected into TRIzol.

343

344 ***Statistics***

345 Unpaired Students T-Test was used to determine statistical significance with two
346 experimental groups, and One-Way ANOVA with Tukey correction was used for
347 experimental groups ≥3. X^2 test was performed to compare distribution across 2 groups.
348 All statistical tests and graphs were made using the Prism 9.4.1 software (GraphPad
349 Software) and are described in relevant Figure Legends.

350

351 **RESULTS**

352

353 **Laminar flow-exposed endothelial cells have a distinct transcriptional profile**

354 Endothelial cells exposed to laminar shear stress exhibit alignment to the flow
355 vector and reduced proliferation, hallmarks of vascular homeostasis or quiescence[1,2,5].
356 To determine whether endothelial cells exposed to laminar flow were transcriptionally
357 quiescent, we utilized a published quiescence score formula generated in non-
358 endothelial epithelial cells[34] and applied it to a scRNAseq dataset we previously

359 generated in primary endothelial cells (HUVEC, human umbilical vein endothelial cells)
360 exposed to laminar flow[8]. This analysis revealed that endothelial cells exposed to
361 homeostatic laminar flow (here called Flow-Maintenance (Flow-M) (15d/cm^2, 72h)) had
362 a significantly higher score than non-flowed control endothelial cells **(Fig. 1A)**. Previous
363 transcriptional characterization revealed 9 clusters primarily separated by flow condition,
364 and the cluster containing the majority of cells exposed to flow (Flow Cluster 1) had a
365 significantly higher epithelial quiescence score compared to the equivalent control
366 cluster (Static Cluster 1), indicating that this quiescence score positively correlates with
367 flow-exposed endothelial cells predicted to be quiescent. Quiescence score
368 comparisons among minor flow clusters showed heterogeneity relative to Flow Cluster
369 1, and a similar comparison of static clusters also revealed heterogeneity relative to
370 Static Cluster 1, indicating that distinct clusters exhibit quiescence heterogeneity. As
371 predicted, Flow Cluster 2, Static Cluster 2, and Mix Cluster (endothelial cells from flow
372 and static conditions), previously defined as proliferative populations[8], had a
373 significantly reduced quiescence score **(Fig. 1A).**
374
375 We next used the scRNA seq dataset to generate an independent endothelial
376 quiescence score algorithm. Since a hallmark of cellular quiescence is downregulation
377 of proliferation markers and upregulation of cell cycle inhibitors[18], this score was
378 primarily generated using expression levels of cell cycle genes that were down- or
379 upregulated in endothelial cells exposed to homeostatic laminar flow (Flow-M) **(Supp.**
380 **Table 1)**. The endothelial quiescence score was then applied to the dataset to verify
381 that the score predicted the relationships. Consistent with the epithelial score, Flow

382 Cluster 1 had a significantly higher quiescence score compared to Static Cluster 1, and
383 the proliferation-associated clusters associated had significantly lower scores **(Fig. 1B).**
384 These findings indicate that endothelial cells exposed to homeostatic laminar flow
385 (Flow-M) are in a transcriptionally quiescent cell cycle state.
386
387 Non-endothelial cells exposed to different quiescence stimuli have unique
388 transcriptional profiles[16,18], so we hypothesized that the mode of quiescence induction
389 affects the quiescence score of endothelial cells. Application of the endothelial
390 quiescence score algorithm to HUVEC bulk RNAseq data showed significant increases
391 under flow and high density compared to static and low-density conditions, respectively
392 **(Fig. 1C)**, and these relationships held when the epithelial quiescence score algorithm
393 was applied **(Supp. Fig. 1A)**. Venn diagrams revealed that homeostatic laminar flow
394 (Flow-M) and contact inhibition have both distinct and shared transcriptional changes in
395 endothelial cells, with approximately 25% of regulated genes shared for up- and down-
396 regulated categories (upregulated: 21.7% (494/2272) flow and 24.3% (494/2030)
397 density shared genes; down-regulated 25.1% (573/2282) flow and 23.7% (573/2415)
398 density shared genes) **(Supp. Fig. 1B)**. Further analysis of highly differentially
399 expressed genes revealed only one overlapping gene (*CCDC190*) that was
400 downregulated between flow and high-density conditions, and no genes were highly
401 upregulated with both flow and high density conditions, indicating that the quiescence
402 profiles of endothelial cells exposed to extended laminar flow or high density are largely
403 distinct **(Supp. Fig. 1C-F)**. Further analysis revealed that expression of cell cycle
404 activators was down-regulated regardless of quiescence induction stimulus, while cell

405 cycle inhibitor expression showed an increased trend with high density but not with
406 homeostatic flow **(Fig. 1D-E).** Thus, endothelial cells respond to homeostatic laminar
407 flow exposure with a distinct quiescence transcriptional profile compared to high
408 density-induced quiescence that includes differences in how cell cycle inhibitors are
409 regulated, suggesting unique properties of flow-mediated endothelial cell quiescence.
410

411 **Shallow quiescence depth characterizes endothelial cells exposed to extended**
412 **laminar flow**

413 Quiescence depth, as defined by time to cell cycle reentry upon stimulus
414 removal, varies in non-endothelial cells[22–24]. Because cell cycle inhibitor expression was
415 not upregulated in endothelial cells exposed to laminar flow, we hypothesized that they
416 are in a relatively shallow quiescence state. We assessed quiescence depth by
417 measuring cell cycle reentry time after quiescence stimulus removal, via EdU labeling
418 and pRB (phospho-retinoblastoma protein) expression **(Supp. Fig. 2A)**[37,38]. EdU labels
419 cells in S-phase, and phosphorylation releases RB from E2F and permits progression
420 through the G_1-S checkpoint and proliferation[38,39]. Endothelial cells exposed to
421 homeostatic laminar flow (Flow-M) or contact inhibition had significantly reduced EdU-
422 labeled **(Fig. 2A-B, D-E)** and pRB+ cells **(Fig. 2A, C, D, F; Supp. Fig 2B-C)** at the end
423 of the flow or contact inhibition period, consistent with previously published work[7,12,40].
424 HUVEC released from homeostatic flow (Flow-M) significantly increased EdU-labeled
425 and pRB+ cells within 2h of flow cessation, while release from contact inhibition only
426 showed significant increases in EdU-labeling and pRB reactivity 8h post-release **(Fig.**
427 **2A-F, Supp. Fig. 2B-C)**, and HAEC (human aortic endothelial cells) showed similar

428 stimulus-dependent differences in quiescence depth **(Supp. Fig. 2D-G)**. Thus,
429 endothelial cells exposed to homeostatic laminar flow (Flow-M) are less deeply
430 quiescent compared to contact-inhibited cells, independent of endothelial subtype.
431

432 **Cell cycle inhibitor p27 expression correlates with quiescence depth and is**
433 **required for flow-mediated quiescence**

434 The cell cycle inhibitor p27 (*CDKN1B*) is often upregulated with quiescence in
435 non-endothelial cells[41–43], so we analyzed endothelial p27 expression and found a
436 highly significant decrease in *CDKN1B* RNA expression and p27+ HUVEC after
437 exposure to homeostatic Flow-M **(Fig. 3A-C; Supp. Fig 3A,C)**. In contrast, we
438 confirmed that p27 RNA and protein levels significantly increased in contact inhibited
439 HUVEC[40] **(Fig. 3D-F; Supp. Fig. 3B-C)**, and HAEC also had reduced p27+ cells after
440 exposure to homeostatic Flow-M **(Supp. Fig. 3D-E)**. Taken together, these findings
441 show that p27 expression positively correlates with quiescence depth in endothelial
442 cells, independent of endothelial subtype.
443
444
445 We interrogated p27 function in endothelial flow-mediated quiescence via siRNA
446 knockdown (KD) and found that p27 depletion and exposure to homeostatic flow (Flow-
447 M) significantly increased EdU-labeling and staining for Ki67, a marker of cells in
448 $S/G_2/M$[44], over controls **(Fig. 4A-B; Supp. Fig. 3F-H)**. Transcriptional profiling of
449 quiescent endothelial cells depleted for p27 under homeostatic flow or high density
450 revealed little overlap in the profiles of genes up- or down-regulated between conditions
451 (upregulated: 9.0% (12/133) flow and 8.6% (12/139) density shared genes; down-

452 regulated 13.4% (18/134) flow and 0.4% (18/313) density shared genes) **(Supp. Fig.**
453 **4A)**. Further analysis of highly differentially expressed genes revealed no overlap
454 between p27 depleted cells and controls in either condition, and gene ontology (GO)
455 comparison revealed no shared terms in either condition **(Supp. Fig. 4B-I)**. These
456 findings indicate that p27 is required for endothelial cell flow-mediated quiescence and
457 affects transcriptional quiescence programs in a quiescence stimulus-dependent
458 manner.
459

460 **p27 regulates endothelial quiescence parameters *in vivo***

461 We asked whether p27 affects vascular processes *in vivo* and hypothesized that
462 p27 loss would deregulate the endothelial cell cycle and angiogenic expansion. We
463 generated a *cdkn1bb* (zebrafish p27 gene) mutant zebrafish line and found significant
464 increases in expression of cell cycle regulators Ki67 *(miKi67*), PCNA *(pcna)* and
465 CyclinD1 *(ccnd1)* in enriched endothelial cell populations from mutant embryos that had
466 reduced p27 (*cdkn1bb)* **(Fig. 4C-F)**. Analysis of vascular sprouting in *cdkn1bb*$^{-/-}$ fish
467 revealed increased ectopic sprouts in the trunk vasculature that was phenocopied by
468 morphant fish depleted for *cdkn1bb* **(Fig. 4G-H, K-L).** Regional quantification of ectopic
469 sprouts along the anterior-posterior axis revealed that mutant or morphant embryos had
470 more ectopic sprouts in the anterior position **(Fig. 4I-J, M)**, suggesting that effects of
471 p27 loss are more associated with mature vascular regions that are likely transitioning
472 to homeostasis. Thus, p27 is required for endothelial cell cycle regulation and proper
473 sprouting *in vivo* and likely affects quiescence establishment.
474

475 **Flow-mediated quiescence depth is temporally regulated in endothelial cells**
476
477 Since p27 is required for flow-mediated endothelial cell quiescence despite very
478 low expression at 72h (Flow-M), we hypothesized that p27 levels temporally fluctuated
479 with flow and found that p27+ cells significantly increased 16h after flow initiation,
480 consistent with another study[45], and then decreased over time to almost undetectable
481 levels at 72h **(Fig. 5A-B, Supp. Fig. 5A).** Another CIP-KIP family cell cycle inhibitor,
482 p21, showed a similar decrease in expression even earlier in the flow time course **(Fig.**
483 **5A,C, Supp. Fig. 5B)**, and Ki67+ cells decreased to almost undetectable levels over
484 flow time **(Fig. 5A,D; Supp. Fig. 5C)**, consistent with the conclusion that endothelial
485 cells leave the cell cycle and become quiescent by 16-24h of laminar flow, then
486 subsequently down-regulate p27 levels while maintaining quiescence.
487
488 We then asked whether endothelial cell quiescence depth was temporally
489 regulated under laminar flow. After 16h of flow (flow establishment (Flow-E)), HUVEC
490 only showed significant EdU-labeling and pRB reactivity 8h post-flow, similar to cells
491 released from contact inhibition and longer than the 2h cell cycle reentry time exhibited
492 by cells exposed to homeostatic flow (Flow-M) **(Fig. 5E-G; Supp. Fig. 5D)**. HAEC also
493 displayed delayed cell cycle reentry post Flow-E, as measured by EdU+ labeling **(Supp.**
494 **Fig. 5E-F)**. These findings correlate with temporal regulation of p27 levels over the flow
495 period and indicate that endothelial cells initially respond to laminar flow with p27
496 upregulation and establishment of a relatively “deep” quiescence (Flow-E) that over time
497 becomes shallower, along with reduced levels of cell cycle inhibitors p27 and p21.

498 Consistent with this idea, endothelial cells were not aligned after 16h flow (Flow-E) but
499 were aligned by 72h (Flow-M) under our flow conditions **(Supp. Fig. 5G-H).**
500
501 We further analyzed the relationship of endothelial quiescence and p27, via
502 single-cell image analysis of endothelial cells exposed to Flow-E or high density and
503 labeled with EdU and p27 reactivity at time points post-flow. Using a threshold for each
504 label, no EdU+/p27+ cells were observed. With time post-flow, p27+/EdU- cells
505 increased and then decreased while p27-/EdU+ cells increased, and with release from
506 contact inhibition similar trends showed that p27+/EdU- cells were replaced by p27-
507 /EdU+ cells over time **(Fig. Supp. 5I-J).** Functionally, endothelial cells with p27
508 depletion had elevated EdU labeling after 16h flow (Flow-E) **(Fig. 5H-I),** consistent with
509 a previous report[45]. These findings indicate that endothelial cell quiescence depth
510 positively correlates with p27 levels during the transition from deep to shallow
511 quiescence, and that individual cells with low p27 expression become competent to
512 reenter the cell cycle.
513
514 **Transcriptional targets of flow-mediated endothelial cell signaling regulate p27**
515 **levels under laminar flow**
516
517 To better understand how endothelial cell p27 may regulate quiescence depth,
518 we examined genes upregulated by laminar flow whose encoded proteins
519 transcriptionally repress p27. Both Notch and BMP signaling are upregulated with
520 laminar flow[2,9,10], and *HES1* and *ID3* are downstream targets of these pathways that
521 transcriptionally repress *CDKN1B* expression via direct and indirect promoter

522 interactions[46,47]. Homeostatic flow (Flow-M) led to *HES1* and *ID3* RNA accumulation in
523 HUVEC **(Supp. Fig. 6A-B)**, and depletion of either *HES1* or *ID3* RNA prevented the
524 normal decrease in p27+ cells under homeostatic laminar flow (Flow-M) in both HUVEC
525 and HAEC **(Fig. 6A-B; Supp. Fig. 6C-E)**, indicating that these repressors are required
526 for flow-mediated reduction of p27 levels over time. Notch signaling is required for
527 endothelial flow-mediated quiescence[45,48], and consistent with this relationship,
528 *NOTCH1* or *DLL4* depletion led to increased EdU+ cells after 16h flow (Flow-E)
529 compared to control **(Supp. Fig. 6F-G)**.
530
531 We hypothesized that *HES1* and *ID3* mediate the temporal changes to
532 endothelial cell quiescence depth and predicted that *HES1* or *ID3* depletion would
533 prevent transition from deep to shallow quiescence. *HES1* and *ID3* expression were
534 significantly increased in cells exposed to Flow-M vs. Flow-E **(Fig. 6C-D)**, and either
535 *HES1* or *ID3* depletion significantly extended the time required for significant increases
536 in EdU+ and pRB+ endothelial cells after Flow-M **(Fig. 6E-J, Supp. Fig. 6H-I),**
537 suggesting that the normal temporal change to shallow quiescence was prevented
538 when these p27 repressors were depleted. These findings are consistent with the idea
539 that endothelial quiescence depth is temporally regulated from deep to shallow over
540 time in conjunction with laminar flow-mediated changes, and that p27 regulates the
541 transition downstream of the transcriptional repressors *HES1* and *ID3*.
542
543 **Endothelial cells exposed to venous laminar flow maintain deep quiescence**
544 We asked whether temporal flow-mediated quiescence depth changes depended
545 on the flow vector (shear stress) magnitude, and we predicted that a lower magnitude of

546 flow characteristic of venous flow would be insufficient to repress p27 levels over time.
547 In contrast to arterial laminar flow (15d/cm^2), endothelial cell exposure to venous
548 laminar flow (5d/cm^2) for 72h (Flow-MV) did not decrease p27+ cells and had increased
549 p27 RNA expression over flow time (Flow-EV) **(Fig. 7A-C)**. Consistent with p27 levels,
550 endothelial cells exposed to venous flow required extended time (8h) to significantly
551 increase EdU+ cells associated with cell cycle reentry **(Fig. 7D-G)** at both 16h (Flow-
552 EV) and 72h (Flow-MV), indicating that temporal quiescence depth regulation depends
553 on the magnitude of the flow stimulus.
554
555 Since quiescence depth is linked to p27 levels in flow-exposed cultured cells, and
556 since flow manipulations are imprecise *in vivo*, we used p27 levels as a proxy for
557 quiescence depth *in vivo* and hypothesized that venous vs. arterial comparisons would
558 reveal elevated venous p27 levels. Two endothelial scRNAseq datasets, one from
559 neonatal mouse skin generated by our lab and one from 24hpf zebrafish generated by
560 the Sumanas lab[49], were subjected to UMAP analysis to define artery/vein/capillary
561 clusters **(Fig. 7H, K)**, and we found that *Cdkn1b* (mouse p27 gene) levels trended
562 higher in venous clusters ($p = 0.1304$) compared to arterial clusters **(Fig. 7I-J)** and were
563 highly significantly increased in zebrafish venous clusters **(Fig 7L-M,** $p=0.0001$**)**. These
564 findings show that p27 levels correlate with flow magnitude *in vivo* and suggest that
565 quiescence depth differs with flow magnitude in arteries vs. veins **(Fig. 8)**.
566
567

568 **DISCUSSION**

569 Flow-mediated endothelial cell quiescence is important for vascular homeostasis
570 and proper barrier function, but how it is set up and maintained is not well-understood.
571 Here we show that endothelial cell quiescence varies with stimulus and flow magnitude
572 and is temporally regulated under flow. We also confirm a functional requirement for the
573 cell cycle inhibitor p27 and find that expression positively correlates with quiescence
574 depth in cells and varies with flow magnitude *in vivo*. Temporal quiescence depth
575 changes under arterial flow require flow-regulated p27 repressors that are targets of
576 flow-mediated pathways such as Notch, suggesting complex regulation of endothelial
577 cell quiescence depth and a model of quiescence regulation **(Fig. 8)**, and they reveal
578 new critical control points for vascular homeostasis[50–52].
579

580 A newly generated endothelial quiescence score tracked well with endothelial
581 cells made quiescent via contact inhibition or homeostatic laminar flow (Flow-M), and
582 application of a published quiescence score developed using different cells and
583 criteria[34] revealed similar trends, indicating that some aspects of vascular quiescence
584 are shared among cell types and conditions. However, further transcriptome analysis
585 revealed stimulus-dependent differences in quiescent endothelial cells, and only contact
586 inhibition broadly stimulated expression of cell cycle inhibitor genes. Further analysis
587 revealed that most differentially regulated genes were unique to the quiescence
588 stimulus, and comparison of highly regulated genes supported that transcriptional
589 profiles are largely unique to the stimulus used to induce quiescence in endothelial
590 cells, similar to patterns in fibroblasts[18].

591 Endothelial cells under homeostatic arterial flow (Flow-M) reentered the cell cycle
592 shortly after flow cessation while contact released cells took significantly longer,
593 indicating distinct quiescence depths associated with quiescence stimulus. Temporal
594 analysis revealed that under Flow-M, that simulates arterial levels of shear stress,
595 endothelial cells first set up a deep quiescence that becomes shallow over flow time,
596 while under Flow-MV, that simulates venous flow, deep quiescence was established in
597 the same time frame but not changed over flow time. This provocative finding suggests
598 that deep quiescence may be important in venous vascular beds that are more poised
599 to proliferate[53,54], to prevent inappropriate cell cycle reentry absent an angiogenic
600 stimulus. It is also in line with a recent study showing that injury-induced collateral
601 vessel expansion originates from arterial endothelial cells[55], and that the inverse
602 correlation of quiescence depth at homeostasis and flow magnitude is linked to
603 interstitial flow where elevated levels are associated with shallower quiescence in
604 fibroblasts[56]. Taken together, these findings suggest complex regulation of quiescence
605 depth relative to flow stimulus.
606
607 Expression of the cell cycle inhibitor p27 positively correlated with quiescence
608 depth in all scenarios, including between homeostatic Flow-M (p27 levels low) vs.
609 contact inhibition (p27 levels high)[40]; between arterial Flow-E (establishment) vs. Flow-
610 M (maintenance) flow times; and between flow magnitude, with lower magnitude
611 venous-type flow associated with elevated p27 levels and deep quiescence across time.
612 This strong correlation was mirrored *in vivo*, as p27 expression was elevated in
613 endothelial cells identified as venous vs. arterial in neonatal mouse ears and zebrafish

614 embryos. We confirmed that p27 is required to establish quiescence in cultured
615 endothelial cells[45] independent of flow magnitude, and we found that p27 loss leads to
616 cell cycle mis-regulation and expanded sprouting *in vivo*, indicating that p27 regulates
617 quiescence establishment and depth in physiological angiogenesis.
618
619 The temporal fluctuations in quiescence depth and p27 levels under arterial flow
620 link to *HES1* and *ID3*, flow-regulated[9,10] transcriptional repressors of p27[57–59]
621 downstream of Notch and BMP signaling, respectively. Both repressors are functionally
622 required non-redundantly to dampen p27 expression as endothelial cells move from
623 quiescence establishment to maintenance and vascular homeostasis, and their
624 expression increases with flow time as cells transition from establishment to
625 maintenance. Quiescence depth under arterial flow is more profound in the absence of
626 either repressor, suggesting that increased Notch and BMP signaling during
627 establishment, and subsequent upregulation of these repressors leads to reduced p27
628 expression levels and a change from a deep to shallow endothelial quiescence depth
629 **(Fig. 8).** This model suggests that in addition to p27-mediated cell cycle regulation in
630 early vascular development to promote arterio-venous differentiation[45,60], p27 is
631 important for subsequent modulation of endothelial quiescence depth.
632
633 What might be an advantage to endothelial cells in a shallow quiescence state
634 under arterial flow maintenance (homeostasis) conditions? One possibility is protection
635 from premature permanent arrest, called senescence[61]. Quiescent fibroblasts eventually
636 undergo senescence[62], and fibroblast *HES1* expression prevents premature

637 senescence[63]. Senescent arterial endothelial cells often express a senescence-
638 associated secretory phenotype (SASP)[64] characterized by inflammatory cytokine
639 expression that contributes to endothelial dysfunction, leading to cardiovascular
640 disease[65]. Thus, arterial endothelial cells in a shallow quiescence state may be
641 protected from inappropriate senescence, while the deeper quiescence of venous
642 endothelial cells may help prevent inappropriate cell cycle reentry. Thus, our findings
643 that endothelial flow-mediated quiescence regulation is linked to p27 suggest potential
644 new therapeutic targets for vascular dysfunction.
645

646 **ACKNOWLEDGMENTS**

647
648 We thank members of the Bautch and Cook labs for their support and feedback, the
649 UNC High Throughput Sequencing Core for technical help, and the UNC Flow
650 Cytometry Core for FACs sorting. We thank BioRender for figure model generation.
651

652 **AUTHOR CONTRIBUTIONS**

653 Natalie T Tanke (NTT), Jeanette Gowen Cook (JGC), Victoria L Bautch (VLB)
654 conceptualized the work; NTT, Ziqing Liu (ZL), Michaelanthony T Gore (MTG), Pauline
655 Bougaran (PB), Allison Marvin (AM), Mary B Linares (MBL), Arya Sharma (AS), Morgan
656 Oatley (MO), Tianji Yu (TY), Kaitlyn Quigley (KQ), and Sarah Vest (SV) performed and
657 analyzed experiments. NTT and VLB wrote and edited the manuscript; VLB and JGC
658 provided study supervision and oversight.
659
660
661

FUNDING

This work was supported by grants from the National Institutes of Health (R35 HL139950 and GM129074 to VLB), the MiBioX T32 Training Grant (T32 GM 119999-03), a Ruth L. Kirschstein Predoctoral Fellowship (1F31HL156527-01 to NTT), and an American Heart Association Postdoctoral Fellowship (AHA829371 to MO).

DECLARATION OF INTERESTS: none

672 **REFERENCES**
673

674 1. Privratsky JR, Newman PJ. PECAM-1: regulator of endothelial junctional integrity.
675 *Cell Tissue Res*. 2014;355(3):607-619. doi:10.1007/s00441-013-1779-3

676 2. Baeyens N, Schwartz MA. Biomechanics of vascular mechanosensation and
677 remodeling. *Mol Biol Cell*. 2016;27(1):7-11. doi:10.1091/mbc.E14-11-1522

678 3. Sluysmans S, Vasileva E, Spadaro D, Shah J, Rouaud F, Citi S. The role of apical
679 cell-cell junctions and associated cytoskeleton in mechanotransduction. *Biol Cell*.
680 2017;109(4):139-161. doi:10.1111/boc.201600075

681 4. Levesque MJ, Sprague EA, Schwartz CJ, Nerem RM. The Influence of Shear
682 Stress on Cultured Vascular Endothelial Cells: The Stress Response of an
683 Anchorage-Dependent Mammalian Cell. *Biotechnol Prog*. 1989;5(1):1-8.
684 doi:10.1002/btpr.5420050105

685 5. Levesque MJ, Nerem RM, Sprague EA. Vascular endothelial cell proliferation in
686 culture and the influence of flow. *Biomaterials*. 1990;11(9):702-707.
687 doi:10.1016/0142-9612(90)90031-k

688 6. Ziegler T, Nerem RM. Effect of flow on the process of endothelial cell division.
689 *Arterioscler Thromb J Vasc Biol*. 1994;14(4):636-643. doi:10.1161/01.atv.14.4.636

690 7. Ruter DL, Liu Z, Ngo KM, X S, Marvin A, Buglak DB, Kidder EJ, Bautch VL.
691 SMAD6 transduces endothelial cell flow responses required for blood vessel
692 homeostasis. *Angiogenesis*. 2021;24(2):387-398. doi:10.1007/s10456-021-09777-7

693 8. Liu Z, Ruter DL, Quigley K, Tanke NT, Jiang Y, Bautch VL. Single-Cell RNA
694 Sequencing Reveals Endothelial Cell Transcriptome Heterogeneity Under
695 Homeostatic Laminar Flow. *Arterioscler Thromb Vasc Biol*. 2021;41(10):2575-
696 2584. doi:10.1161/ATVBAHA.121.316797

697 9. Yang J, Li X, Li Y, Southwood M, Ye L, Long L, Al-Lamki RS, Morrell NW. Id
698 proteins are critical downstream effectors of BMP signaling in human pulmonary
699 arterial smooth muscle cells. *Am J Physiol - Lung Cell Mol Physiol*.
700 2013;305(4):L312-L321. doi:10.1152/ajplung.00054.2013

701 10. Jouve C, Palmeirim I, Henrique D, Beckers J, Gossler A, Ish-Horowicz D, Pourquie
702 O. Notch signalling is required for cyclic expression of the hairy-like gene HES1 in
703 the presomitic mesoderm. *Development*. 2000;127(7):1421-1429.
704 doi:10.1242/dev.127.7.1421

705 11. Caplan BA, Schwartz CJ. Increased endothelial cell turnover in areas of in vivo
706 Evans Blue uptake in the pig aorta. *Atherosclerosis*. 1973;17(3):401-417.
707 doi:10.1016/0021-9150(73)90031-2

12. Schlereth K, Weichenhan D, Bauer T, Heumann T, Giannakouri E, Lipka D, Jaeger S, Schlesner M, Aloy P, Eils R, Plass C, Augustin HG. The transcriptomic and epigenetic map of vascular quiescence in the continuous lung endothelium. *eLife*. 2018;7:e34423. doi:10.7554/eLife.34423

13. Millauer B, Wizigmann-Voos S, Schnürch H, Martinez R, Møller NPH, Risau W, Ullrich A. High affinity VEGF binding and developmental expression suggest Flk-1 as a major regulator of vasculogenesis and angiogenesis. *Cell*. 1993;72(6):835-846. doi:10.1016/0092-8674(93)90573-9

14. Gerhardt H, Golding M, Fruttiger M, Ruhrberg C, Lundkvist A, Abramsson A, Jeltsch M, Mitchell C, Alitalo K, Shima D, Betsholtz C. VEGF guides angiogenic sprouting utilizing endothelial tip cell filopodia. *J Cell Biol*. 2003;161(6):1163-1177. doi:10.1083/jcb.200302047

15. Bernatchez PN, Soker S, Sirois MG. Vascular Endothelial Growth Factor Effect on Endothelial Cell Proliferation, Migration, and Platelet-activating Factor Synthesis Is Flk-1-dependent *. *J Biol Chem*. 1999;274(43):31047-31054. doi:10.1074/jbc.274.43.31047

16. Min M, Spencer SL. Spontaneously slow-cycling subpopulations of human cells originate from activation of stress-response pathways. *PLoS Biol*. 2019;17(3):e3000178. doi:10.1371/journal.pbio.3000178

17. Johnson MS, Cook JG. Cell cycle exits and U-turns: Quiescence as multiple reversible forms of arrest. *Fac Rev*. 2023;12:5. doi:10.12703/r/12-5

18. Coller HA, Sang L, Roberts JM. A New Description of Cellular Quiescence. *PLOS Biol*. 2006;4(3):e83. doi:10.1371/journal.pbio.0040083

19. Hartwell LH, Culotti J, Pringle JR, Reid BJ. Genetic Control of the Cell Division Cycle in Yeast. *Science*. 1974;183(4120):46-51. doi:10.1126/science.183.4120.46

20. Tarn WY, Lai MC. Translational control of cyclins. *Cell Div*. 2011;6:5. doi:10.1186/1747-1028-6-5

21. Minshull J, Pines J, Golsteyn R, Standart N, Mackie S, Colman A, Blow J, Ruderman JV, Wu M, Hunt T. The role of cyclin synthesis, modification and destruction in the control of cell division. *J Cell Sci*. 1989;1989(Supplement_12):77-97. doi:10.1242/jcs.1989.Supplement_12.8

22. Kwon JS, Everetts NJ, Wang X, Wang W, Croce KD, Xing J, Yao G. Controlling Depth of Cellular Quiescence by an Rb-E2F Network Switch. *Cell Rep*. 2017;20(13):3223-3235. doi:10.1016/j.celrep.2017.09.007

23. Fujimaki K, Li R, Chen H, Croce KD, Zhang HH, Xing J, Bai F, Yao G. Graded regulation of cellular quiescence depth between proliferation and senescence by a

lysosomal dimmer switch. *Proc Natl Acad Sci*. Published online October 21, 2019. doi:10.1073/pnas.1915905116

24. Rodgers JT, King KY, Brett JO, Cromie MJ, Charville GW, Maguire KK, Brunson C, Mastey N, Liu L, Tsai CR, Goodell MA, Rando TA. mTORC1 controls the adaptive transition of quiescent stem cells from G0 to GAlert. *Nature*. 2014;510(7505):393-396. doi:10.1038/nature13255

25. Min M, Rong Y, Tian C, Spencer SL. Temporal integration of mitogen history in mother cells controls proliferation of daughter cells. *Science*. 2020;368(6496):1261-1265. doi:10.1126/science.aay8241

26. Schindelin J, Arganda-Carreras I, Frise E, Kaynig V, Longair M, Pietzsch T, Preibisch S, Rueden C, Saalfeld S, Schmid B, Tinevez JY, White DJ, Hartenstein V, Eliceiri K, Tomancak P, Cardona A. Fiji: an open-source platform for biological-image analysis. *Nat Methods*. 2012;9(7):676-682. doi:10.1038/nmeth.2019

27. Dardik A, Chen L, Frattini J, Asada H, Aziz F, Kudo FA, Sumpio BE. Differential effects of orbital and laminar shear stress on endothelial cells. *J Vasc Surg*. 2005;41(5):869-880. doi:10.1016/j.jvs.2005.01.020

28. Liang D, Chang JR, Chin AJ, Smith A, Kelly C, Weinberg ES, Ge R. The role of vascular endothelial growth factor (VEGF) in vasculogenesis, angiogenesis, and hematopoiesis in zebrafish development. *Mech Dev*. 2001;108(1):29-43. doi:10.1016/S0925-4773(01)00468-3

29. Mahmood T, Yang PC. Western Blot: Technique, Theory, and Trouble Shooting. *North Am J Med Sci*. 2012;4(9):429-434. doi:10.4103/1947-2714.100998

30. Buglak DB, Bougaran P, Kulikauskas MR, Liu Z, Monaghan-Benson E, Gold AL, Marvin AP, Burciu A, Tanke NT, Oatley M, Ricketts SN, Kinghorn K, Johnson BN, Shiau CE, Rogers S, Guilluy C, Bautch VL. Nuclear SUN1 stabilizes endothelial cell junctions via microtubules to regulate blood vessel formation. Koh GY, Akhmanova A, eds. *eLife*. 2023;12:e83652. doi:10.7554/eLife.83652

31. Dobin A, Davis CA, Schlesinger F, Drenkow J, Zaleski C, Jha S, Batut P, Chaisson M, Gingeras TR. STAR: ultrafast universal RNA-seq aligner. *Bioinforma Oxf Engl*. 2013;29(1). doi:10.1093/bioinformatics/bts635

32. Putri GH, Anders S, Pyl PT, Pimanda JE, Zanini F. Analysing high-throughput sequencing data in Python with HTSeq 2.0. *Bioinforma Oxf Engl*. 2022;38(10):2943-2945. doi:10.1093/bioinformatics/btac166

33. Love MI, Huber W, Anders S. Moderated estimation of fold change and dispersion for RNA-seq data with DESeq2. *Genome Biol*. 2014;15(12):550. doi:10.1186/s13059-014-0550-8

780 34. Wiecek AJ, Cutty SJ, Kornai D, Parreno-Centeno M, Gourmet LE, Tagliazucchi
781 GM, Jacobson DH, Zhang P, Xiong L, Bond GL, Barr AR, Secrier M. Genomic
782 hallmarks and therapeutic implications of G0 cell cycle arrest in cancer. *Genome*
783 *Biol*. 2023;24(1):128. doi:10.1186/s13059-023-02963-4

784 35. Hoshijima K, Jurynec MJ, Klatt Shaw D, Jacobi AM, Behlke MA, Grunwald DJ.
785 Highly Efficient CRISPR-Cas9-Based Methods for Generating Deletion Mutations
786 and F0 Embryos that Lack Gene Function in Zebrafish. *Dev Cell*. 2019;51(5):645-
787 657.e4. doi:10.1016/j.devcel.2019.10.004

788 36. Bresciani E, Broadbridge E, Liu PP. An efficient dissociation protocol for generation
789 of single cell suspension from zebrafish embryos and larvae. *MethodsX*.
790 2018;5:1287-1290. doi:10.1016/j.mex.2018.10.009

791 37. Pereira PD, Serra-Caetano A, Cabrita M, Bekman E, Braga J, Rino J, Santus R,
792 Filipe PL, Sousa AE, Ferreira JA. Quantification of cell cycle kinetics by EdU (5-
793 ethynyl-2′-deoxyuridine)-coupled-fluorescence-intensity analysis. *Oncotarget*.
794 2017;8(25):40514-40532. doi:10.18632/oncotarget.17121

795 38. Goodrich DW, Wang NP, Qian YW, Lee EY, Lee WH. The retinoblastoma gene
796 product regulates progression through the G1 phase of the cell cycle. *Cell*.
797 1991;67(2):293-302. doi:10.1016/0092-8674(91)90181-w

798 39. Buck SB, Bradford J, Gee KR, Agnew BJ, Clarke ST, Salic A. Detection of S-phase
799 cell cycle progression using 5-ethynyl-2′-deoxyuridine incorporation with click
800 chemistry, an alternative to using 5-bromo-2′-deoxyuridine antibodies.
801 *BioTechniques*. 2008;44(7):927-929. doi:10.2144/000112812

802 40. Noseda M, Chang L, McLean G, Grim JE, Clurman BE, Smith LL, Karsan A. Notch
803 activation induces endothelial cell cycle arrest and participates in contact inhibition:
804 role of p21Cip1 repression. *Mol Cell Biol*. 2004;24(20):8813-8822.
805 doi:10.1128/MCB.24.20.8813-8822.2004

806 41. Oesterle EC, Chien WM, Campbell S, Nellimarla P, Fero ML. p27(Kip1) is required
807 to maintain proliferative quiescence in the adult cochlea and pituitary. *Cell Cycle*
808 *Georget Tex*. 2011;10(8):1237-1248. doi:10.4161/cc.10.8.15301

809 42. Besson A, Gurian-West M, Chen X, Kelly-Spratt KS, Kemp CJ, Roberts JM. A
810 pathway in quiescent cells that controls p27Kip1 stability, subcellular localization,
811 and tumor suppression. *Genes Dev*. 2006;20(1):47-64. doi:10.1101/gad.1384406

812 43. Levenberg S, Yarden A, Kam Z, Geiger B. p27 is involved in N-cadherin-mediated
813 contact inhibition of cell growth and S-phase entry. *Oncogene*. 1999;18(4):869-876.
814 doi:10.1038/sj.onc.1202396

815 44. Miller I, Min M, Yang C, Tian C, Gookin S, Carter D, Spencer SL. Ki67 is a Graded
816 Rather than a Binary Marker of Proliferation versus Quiescence. *Cell Rep*.
817 2018;24(5):1105-1112.e5. doi:10.1016/j.celrep.2018.06.110

818 45. Fang JS, Coon BG, Gillis N, Chen Z, Qiu J, Chittenden TW, Burt JM, Schwartz MA,
819 Hirschi KK. Shear-induced Notch-Cx37-p27 axis arrests endothelial cell cycle to
820 enable arterial specification. *Nat Commun*. 2017;8. doi:10.1038/s41467-017-
821 01742-7

822 46. Chassot AA, Turchi L, Virolle T, Fitsialos G, Batoz M, Deckert M, Dulic V,
823 Meneguzzi G, Buscà R, Ponzio G. Id3 is a novel regulator of p27kip1 mRNA in
824 early G1 phase and is required for cell-cycle progression. *Oncogene*.
825 2007;26(39):5772-5783. doi:10.1038/sj.onc.1210386

826 47. Murata K, Hattori M, Hirai N, Shinozuka Y, Hirata H, Kageyama R, Sakai T, Minato
827 N. Hes1 directly controls cell proliferation through the transcriptional repression of
828 p27Kip1. *Mol Cell Biol*. 2005;25(10):4262-4271. doi:10.1128/MCB.25.10.4262-
829 4271.2005

830 48. Sun JX, Dou GR, Yang ZY, Liang L, Duan JL, Ruan B, Li MH, Chang TF, Xu XY,
831 Chen JJ, Wang YS, Yan XC, Han H. Notch activation promotes endothelial
832 quiescence by repressing MYC expression via miR-218. *Mol Ther Nucleic Acids*.
833 2021;25:554-566. doi:10.1016/j.omtn.2021.07.023

834 49. Gurung S, Restrepo NK, Chestnut B, Klimkaite L, Sumanas S. Single-cell
835 transcriptomic analysis of vascular endothelial cells in zebrafish embryos. *Sci Rep*.
836 2022;12(1):13065. doi:10.1038/s41598-022-17127-w

837 50. Herrera MD, Mingorance C, Rodríguez-Rodríguez R, Alvarez de Sotomayor M.
838 Endothelial dysfunction and aging: an update. *Ageing Res Rev*. 2010;9(2):142-152.
839 doi:10.1016/j.arr.2009.07.002

840 51. Seals DR, Jablonkski KL, Donato AJ. Aging and vascular endothelial function in
841 humans. *Clin Sci Lond Engl 1979*. 2011;120(9):357-375.
842 doi:10.1042/CS2010047652. Donato AJ, Machin DR, Lesniewski LA.
843 Mechanisms of Dysfunction in the Aging Vasculature and Role in Age-Related
844 Disease. *Circ Res*. 2018;123(7):825-848. doi:10.1161/CIRCRESAHA.118.312563

845 53. Red-Horse K, Ueno H, Weissman IL, Krasnow MA. Coronary arteries form by
846 developmental reprogramming of venous cells. *Nature*. 2010;464(7288):549-553.
847 doi:10.1038/nature08873

848 54. Ehling M, Adams S, Benedito R, Adams RH. Notch controls retinal blood vessel
849 maturation and quiescence. *Dev Camb Engl*. 2013;140(14):3051-3061.
850 doi:10.1242/dev.093351

851 55. Arolkar G, Kumar SK, Wang H, Gonzalez KM, Kumar S, Bishnoi B, Rios Coronado
852 PE, Woo YJ, Red-Horse K, Das S. Dedifferentiation and Proliferation of Artery
853 Endothelial Cells Drive Coronary Collateral Development in Mice. *Arterioscler*
854 *Thromb Vasc Biol*. 2023;43(8):1455-1477. doi:10.1161/ATVBAHA.123.319319

855 56. Liu B, Wang X, Jiang L, Xu J, Zohar Y, Yao G. Extracellular Fluid Flow Induces
856 Shallow Quiescence Through Physical and Biochemical Cues. *Front Cell Dev Biol*.
857 2022;10:792719. doi:10.3389/fcell.2022.792719

858 57. Mack JJ, Mosqueiro TS, Archer BJ, Jones WM, Sunshine H, Faas GC, Briot A,
859 Aragón RL, Su T, Romay MC, McDonald AI, Kuo CH, Lizama CO, Lane TF, Zovein
860 AC, Fang Y, Tarling EJ, Vallim TQ de A, Navab M, Fogelman AM, Bouchard LS,
861 Iruela-Arispe ML. NOTCH1 is a mechanosensor in adult arteries. *Nat Commun*.
862 2017;8(1):1620. doi:10.1038/s41467-017-01741-8

863 58. Helle E, Ampuja M, Antola L, Kivelä R. Flow-Induced Transcriptomic Remodeling of
864 Endothelial Cells Derived From Human Induced Pluripotent Stem Cells. *Front*
865 *Physiol*. 2020;11. Accessed April 7, 2023.
866 https://www.frontiersin.org/articles/10.3389/fphys.2020.591450

867 59. Zhang MJ, Pisco AO, Darmanis S, Zou J. Mouse aging cell atlas analysis reveals
868 global and cell type-specific aging signatures. Han JDJ, Tyler JK, Hou L, eds. *eLife*.
869 2021;10:e62293. doi:10.7554/eLife.62293

870 60. Acharya BR, Fang JS, Jeffery ED, Chavkin NW, Genet G, Vasavada H, Nelson EA,
871 Sheynkman GM, Humphries MJ, Hirschi KK. Connexin 37 sequestering of
872 activated-ERK in the cytoplasm promotes p27-mediated endothelial cell cycle
873 arrest. *Life Sci Alliance*. 2023;6(8). doi:10.26508/lsa.202201685

874 61. Hayflick L, Moorhead PS. The serial cultivation of human diploid cell strains. *Exp*
875 *Cell Res*. 1961;25(3):585-621. doi:10.1016/0014-4827(61)90192-6

876 62. Marthandan S, Priebe S, Hemmerich P, Klement K, Diekmann S. Long-Term
877 Quiescent Fibroblast Cells Transit into Senescence. *PLOS ONE*.
878 2014;9(12):e115597. doi:10.1371/journal.pone.0115597

879 63. Sang L, Coller HA, Roberts JM. Control of the reversibility of cellular quiescence by
880 the transcriptional repressor HES1. *Science*. 2008;321(5892):1095-1100.
881 doi:10.1126/science.1155998

882 64. Han Y, Kim SY. Endothelial senescence in vascular diseases: current
883 understanding and future opportunities in senotherapeutics. *Exp Mol Med*.
884 2023;55(1):1-12. doi:10.1038/s12276-022-00906-w

885 65. Minamino T, Miyauchi H, Yoshida T, Ishida Y, Yoshida H, Komuro I. Endothelial
886 Cell Senescence in Human Atherosclerosis. *Circulation*. 2002;105(13):1541-1544.
887 doi:10.1161/01.CIR.0000013836.85741.17

888

889 **Nonstandard Abbreviations and Acronyms**
890
891 HUVEC: Human Umbilical Vein Endothelial Cells
892 HAEC: Human Aortic Endothelial Cells
893 Flow-M: Flow maintenance; 72 hr 15d/cm^2
894 Flow-E: Flow establishment; 16 hr 15d/cm^2
895 Flow-EV, Flow establishment venous; 16h, 5d/cm^2
896 Flow-MV, Flow maintenance, venous; 16h, 5d/cm^2
897 siRNA: Small interfering RNA
898 KD: Knockdown
899 A.U.: Arbitrary unit
900 pRB: Phospho retinoblastoma protein
901 EdU: 5-Ethynyl-2'-deoxyuridine
902 *HES1*: Hes Family BHLH Transcription Factor 1
903 *ID3*: Inhibitor of DNA Binding 3
904

905 **FIGURE LEGENDS**
906
907 **Figure 1. Laminar flow-mediated quiescence is transcriptionally distinct.**

908 **(A)** Quantification of epithelial quiescence score in HUVEC scRNA dataset by cluster
909 (previously defined[8]). Flow-M, flow maintenance (laminar flow (15d/cm^2/72h)). Static
910 cells were visually checked for subconfluence and collected 48h post-seeding. **(B)**
911 Quantification of endothelial quiescence score in HUVEC scRNA dataset by cluster. **(C)**
912 Endothelial quiescence score on bulk RNA seq data of HUVEC exposed to indicated
913 stimuli, n= 3 replicates. **(D-E)** Heatmaps showing relative expression of cell cycle
914 proliferation markers (green font) and inhibitors (red font) plotted using bulk RNAseq
915 data of HUVEC under indicated conditions, n=3 replicates. Statistics, one-way ANOVA
916 with Tukey's multiple comparison test.
917
918
919 **Figure 2. Endothelial cell flow maintenance quiescence stimulus leads to shallow**
920 **quiescence depth.**

921 **(A)** Representative images of HUVEC under static (non-flow) or Flow-M (flow
922 maintenance) conditions with EdU incorporation and fixation at indicated times post
923 Flow-M release. Cultures stained for DAPI (white, nuclear mask) and EdU (red, S-
924 phase) or pRB (blue, interphase). Scale bar, 50 μm. White arrow, flow direction. **(B)**
925 Quantification of percent EdU+ cells with indicated conditions. n=3 replicates, 5 images
926 per condition per replicate. **(C)** Quantification of percent pRB+ cells with indicated
927 conditions. n=3 replicates, 5 images per condition per replicate. **(D)** Representative
928 images of HUVEC under indicated density conditions with EdU incorporation and
929 fixation at indicated times post high-density release. Cultures stained for DAPI (white,

930 nuclear mask) and EdU (red, S-phase) or pRB (blue, interphase). Scale bar, 50 μm. **(E)**
931 Quantification of percent EdU+ cells with indicated conditions. n=3 replicates, 6 images
932 per condition per replicate. **(F)** Quantification of percent pRB+ cells with indicated
933 conditions. n=3 replicates, 6 images per condition per replicate. Statistics, one-way
934 ANOVA with Tukey's multiple comparisons test.

935
936
937 **Figure 3. Cell cycle inhibitor p27 expression levels vary with endothelial**
938 **quiescence stimulus.**
939 **(A)** RT-qPCR for *CDKN1B* levels under indicated conditions. n=3 replicates. **(B)**
940 Representative images of HUVEC under indicated conditions stained for p27 (green)
941 and DAPI (white, nuclear mask). Scale bar, 50 μm. White arrow, flow direction. **(C)**
942 Quantification of HUVEC p27+ cells under indicated conditions. n=3 replicates, 5
943 images per condition per replicate. **(D)** RT-qPCR for *CDKN1B* levels under indicated
944 conditions. n=3 replicates. **(E)** Representative images of HUVEC under indicated
945 conditions stained for p27 (green) and DAPI (white, nuclear mask). Scale bar, 50 μm.
946 **(F)** Quantification of HUVEC p27+ cells under indicated conditions. n=3 replicates, 5
947 images per condition per replicate. Statistics, student's two-tailed *t*-test.

948

949 **Figure 4. p27 establishes quiescence in endothelial cells and regulates cell cycle**
950 **and vascular expansion *in vivo*.**
951 **(A)** Representative images of HUVEC with indicated siRNA treatments and conditions.
952 after EdU incorporation (red, S-phase) and staining with DAPI (white, nuclear mask).
953 Scale bar, 50 μm. White arrow, flow direction. **(B)** Quantification of EdU+ cells with

954 indicated conditions. n=3 replicates, 5 images per condition per replicate. **(C-F)** RT-
955 qPCR of FACs sorted 24 hpf zebrafish endothelial cells from *Tg(fli:LifeAct-GFP)* (green,
956 endothelial cell marker) embryos of indicated genotypes for *cdkn1bb* **(C)***, mki67* **(D)***,*
957 *pcna* **(E)***,* and *ccnd1* **(F)** levels. n=3 replicates. **(G)** Representative images of 36hpf
958 *Tg(fli:LifeAct-GFP)* (green, endothelial cell marker) embryos that were also WT or
959 *cdkn1bb*$^{-/-}$. Yellow arrows, ectopic sprouts. Scale bar, 50 µm. **(H)** Quantification of
960 ectopic sprouts per embryo. n=3 replicates, 5 images per condition per replicate. **(I)**
961 Diagram defining regions for ectopic sprout quantification in embryonic zebrafish. **(J)**
962 Quantification of % ectopic sprouts in *Tg(fli:LifeAct-GFP)* (green, endothelial cell
963 marker) embryos and of indicated genotypes per region. n=3 replicates, 5 images per
964 condition per replicate. **(K)** Representative images of 36hpf *Tg(fli:LifeAct-GFP)* embryos
965 injected with control (NT) or cdkn1bb MO at the one-cell stage. Yellow arrows, ectopic
966 sprouts. Scale bar, 50 µm. **(L)** Quantification of ectopic sprouts per embryo. n=3
967 replicates, 5 images per condition per replicate. **(M)** Quantification of % ectopic sprouts
968 in *Tg(fli:LifeAct-GFP)* (green, endothelial cell marker) and with indicated MO injection
969 per region. n=3 replicates, 5 images per condition per replicate. Statistics, student's two-
970 tailed *t*-test (C-F, H, L), one-way ANOVA with Tukey's multiple comparisons test (B),
971 and X^2 test (J, M).
972
973

974 **Figure 5. Endothelial quiescence depth varies with laminar flow exposure time**
975 **and positively correlates with p27 expression levels.**
976 **(A)** Representative images of HUVEC with indicated conditions and stained for p27
977 (inhibitor), p21 (inhibitor), Ki67 (proliferation marker), and DAPI (nucleus) in white. Scale
978 bar, 50 μm. White arrow, flow direction. **(B-D)** Quantification of percent p27+ (**B**), p21+
979 cells (**C**), or Ki67+ cells (**D**). n=3 replicates, 5 images per condition per replicate. **(E)**
980 Representative images of HUVEC under indicted conditions and after EdU incorporation
981 (red, S-phase) and stained for pRB (blue, interphase) and with DAPI (white, nuclear
982 mask), Flow-E, flow establishment (15d/cm^2, 16h); Flow-M, flow maintenance (15d/cm^2,
983 72h). Scale bar, 50 μm. White arrow, flow direction. **(F)** Quantification of EdU+ cells
984 under indicated conditions. n=3 replicates, 5 images per condition per replicate. **(G)**
985 Quantification of pRB+ cells under indicated conditions. n=3 replicates, 5 images per
986 condition per replicate. **(H)** Representative images of HUVEC with indicated siRNA
987 treatments and conditions after EdU incorporation (red, S-phase) and staining with
988 DAPI (white, nuclear mask). Scale bar, 50 μm. White arrow, flow direction. **(I)**
989 Quantification of EdU+ cells with indicated conditions. n=3 replicates, 5 images per
990 condition per replicate. Statistics, one-way ANOVA with Tukey's multiple comparisons
991 test.
992
993

994 **Figure 6. BMP and NOTCH regulated p27 repressors *HES1* and *ID3* regulate p27**
995 **levels and flow-mediated quiescence depth.**
996 **(A)** Representative images of HUVEC under indicated conditions and with indicated
997 siRNA treatment. Cells stained for p27 (green) and DAPI (white, nuclear mask). Scale
998 bar, 50 μm. White arrow, flow direction. **(B)** Quantification of p27+ cells under indicated
999 conditions and treatments. n=3 replicates, 5 images per condition per replicate. **(C-D)**
1000 RT-qPCR for *HES1* **(C)** and *ID3* **(D)** levels under indicated conditions. n=3 replicates.
1001 **(E)** Representative images of HUVEC under indicated conditions and siRNA treatments.
1002 Cells were labeled with EdU (red, S-phase) and stained for pRB (blue, interphase) and
1003 DAPI (white, nuclear mask). Scale bar, 50 μm. White arrow, flow direction. **(F)**
1004 Quantification of EdU+ cells with indicated conditions. n=3 replicates, 5 images per
1005 condition per replicate. **(G)** Quantification of pRB+ cells with indicated conditions. n=3
1006 replicates, 5 images per condition per replicate. **(H)** Representative images of HUVEC
1007 under indicated conditions and siRNA treatments. Cells were labeled with EdU (red, S-
1008 phase) and stained for pRB (blue, interphase) and DAPI (white, nuclear mask). Scale
1009 bar, 50 μm. White arrow, flow direction. **(I)** Quantification of EdU+ cells under indicated
1010 conditions. n=3 replicates, 5 images per condition per replicate. **(J)** Quantification of
1011 pRB+ cells under indicated conditions. n=3 replicates, 5 images per condition per
1012 replicate. Statistics, student's two-tailed *t*-test (C-D) and one-way ANOVA with Tukey's
1013 multiple comparisons test (B, F-G, I-J).
1014
1015
1016

1017 **Figure 7. Endothelial cells establish and maintain deep quiescence under venous**
1018 **flow and express elevated p27 levels *in vivo*.**
1019 **(A)** Representative images of HUVEC under indicated conditions (Flow-MV (5d/cm^2,
1020 72h)) stained for p27 (green) and DAPI (white, nuclear mask). Scale bar, 50 µm. White
1021 arrow, flow direction. **(B)** Quantification of HUVEC p27+ cells under indicated
1022 conditions, n=3 replicates, 5 images per condition per replicate. **(C)** RT-qPCR for
1023 *CDKN1B* levels in indicated conditions. n=3 replicates. **(D)** Representative images of
1024 HUVEC under static (non-flow) or Flow-EV (5d/cm^2, 16h) conditions with EdU
1025 incorporation and fixation at indicated times post Flow-EV release. Cells stained for
1026 DAPI (white, nuclear mask) and EdU (red, S-phase), Scale bar, 50 µm. White arrow,
1027 flow direction. **(E)** Quantification of EdU+ cells with indicated conditions. n=3 replicates,
1028 5 images per condition per replicate. **(F)** Representative images of HUVEC under static
1029 (non-flow) or Flow-MV conditions (5d/cm^2, 72h) with EdU incorporation and fixation at
1030 indicated times post Flow-MV release. Cells stained for DAPI (white, nuclear mask) and
1031 EdU (red, S-phase), Scale bar, 50 µm. White arrow, flow direction. **(G)** Quantification of
1032 EdU+ cells with indicated conditions. n=3 replicates, 5 images per condition per
1033 replicate. **(H)** UMAP grouping of artery, vein, and capillary endothelial cell clusters
1034 enriched from neonatal mouse ear skin. **(I)** UMAP overlaid with *Cdkn1b (p27)*
1035 expression. **(J)** Dot plot of *Cdkn1b* expression by endothelial sub-type. **(K)** UMAP
1036 grouping of endothelial artery, vein, and capillary clusters reanalyzed from 24hpf
1037 embryonic zebrafish. **(L)** UMAP overlaid with *cdkn1bb (p27)* expression. **(M)** Dot plot of
1038 *Cdkn1b* expression by endothelial sub-type. Statistics, student's two-tailed *t*-test (B-C,
1039 J-M) and one-way ANOVA with Tukey's multiple comparisons test (E, G).

1040 **Figure 8.** ***Model of endothelial cell flow-mediated quiescence depth.***

1041 Proposed model for dynamic regulation of endothelial cell flow-mediated quiescence
1042 depth with flow exposure time and magnitude. In the first 16h (Flow-E, arterial flow
1043 establishment) of laminar flow, a deep quiescence is established accompanied by high
1044 levels of cell cycle inhibitor p27, independent of flow magnitude. With time under arterial
1045 flow (Flow-M, flow maintenance), *HES1* and *ID3* transcription factors are upregulated
1046 downstream of flow-mediated Notch and BMP signaling, and they repress p27
1047 transcription leading to a shallow quiescence depth. Deep quiescence and high p27
1048 levels characterize venous flow establishment at 16h (Flow-EV, venous flow
1049 establishment), and this deep quiescence perdures with time under venous flow (Flow-
1050 MV).

1051

1052 **SUPPLEMENTARY FIGURE LEGENDS**

1053

1054 **Supplemental Figure 1. Endothelial cell quiescence transcriptional profiles are**
1055 **stimulus-dependent.**

1056 **(A)** Quantification using an epithelial quiescence score[34] on HUVEC bulk RNAseq
1057 dataset under different conditions. n=3 replicates. Flow-M, flow maintenance (15d/cm^2,
1058 72h). **(B)** Venn diagrams showing bulk RNA seq analysis of genes up- and down-
1059 regulated in HUVEC under indicated conditions. **(C-F)** Heatmaps showing relative
1060 expression levels of differentially regulated genes (top 50 by fold change and p-value) in
1061 bulk RNA seq from HUVEC under indicated conditions. Statistics, one-way ANOVA with
1062 Tukey's multiple comparisons test.

1063

1064 **Supplemental Figure 2. Quiescence depth is replicated in HAEC (human arterial**
1065 **endothelial cells).**
1066 **(A)** Schematic showing areas of scratch wound used for imaging post-scratch for
1067 contact inhibition quiescence depth experiments. **(B)** Quantification of HUVEC pRB
1068 nuclear fluorescence intensity under indicated conditions. n=3 replicates, 5 images
1069 averaged per condition per replicate. **(C)** Quantification of HUVEC nuclear fluorescence
1070 intensity of pRB in low vs. high density release timepoints. n=3 replicates, 5 averaged
1071 images per condition per replicate. **(D)** Representative images of HAEC under static
1072 (non-flow) or Flow-M (flow maintenance) conditions with EdU incorporation and fixation
1073 at indicated times post Flow-M release. Cells stained for DAPI (white, nuclear mask)
1074 and EdU (red, S-phase). Scale bar, 50 μm. White arrow, flow direction. **(E)**
1075 Quantification of percent EdU+ cells with indicated conditions. n=3 replicates, 5 images
1076 per condition per replicate. **(F)** Representative images of HAEC under indicated density
1077 conditions with EdU incorporation and fixation at indicated times post density release.
1078 Cells stained for DAPI (white, nuclear mask) and EdU (red, S-phase). Scale bar, 50 μm.
1079 **(G)** Quantification of percent EdU+ cells with indicated conditions. n=3 replicates, 5
1080 images per condition per replicate. Statistics, one-way ANOVA with Tukey's multiple
1081 comparisons test.
1082
1083 **Supplemental Figure 3. Cell cycle inhibitor p27 expression differs with**
1084 **quiescence stimulus.**
1085
1086 **(A)** Quantification of p27 nuclear fluorescence intensity in indicated conditions. n=3
1087 replicates, 5 images averaged per condition per replicate. **(B)** Quantification of p27

1088 nuclear fluorescence intensity in indicated conditions. n=3 replicates, 5 images
1089 averaged per condition per replicate. **(C)** Western blot of p27 expression under
1090 indicated conditions, and with indicated antibodies. p27 Ab #1 (Cell Signaling) and p27
1091 Ab #2 (Santa Cruz). **(D)** Representative images of HAEC under indicated conditions
1092 stained for p27 (green) and DAPI (white, nuclear mask). Scale bar, 50 μm. White arrow,
1093 flow direction. **(E)** Quantification of HAEC p27+ cells under indicated conditions, n=3
1094 replicates, 5 images per condition per replicate. **(F)** Representative images of HUVEC
1095 with indicated siRNA and treatments. Endothelial cells stained with Ki67 (yellow,
1096 proliferation marker) and DAPI (gray, nucleus mask). Scale bar 50 μm. White arrow,
1097 flow direction. **(G)** Quantification of percent Ki67+ cells. n=3 replicates, 5 images per
1098 condition per replicate. **(H)** Quantification of nuclear fluorescence intensity of Ki67. n=3
1099 replicates, 5 averaged images per condition per replicate. Statistics, student's two-tailed
1100 *t*-test (A-B, E) and one-way ANOVA with Tukey's multiple comparisons test (G-H).
1101

1102 **Supplemental Figure 4. p27 depletion leads to distinct transcriptional changes**
1103 **dependent on quiescence stimulus.**
1104 **(A)** Venn diagrams showing overlap of HUVEC genes differentially regulated in
1105 indicated conditions and for *CDKN1B* KD compared to NT. **(B-E)** Heatmaps showing
1106 relative expression levels of genes differentially regulated (top 50 by fold change and p-
1107 value) in response to indicated conditions. **(F-I)** GO analysis performed on differentially
1108 expressed genes from bulk RNA-seq data comparing indicated conditions/treatments.
1109 Representative biological processes GO terms significantly enriched (P adjusted < 0.1)
1110 in differentially regulated genes are shown.

1111 **Supplemental Figure 5. Cell cycle inhibitor and Ki67 expression intensity varies**
1112 **with flow and correlates with flow-mediated endothelial cell alignment**.
1113 **(A)** Quantification of p27 nuclear fluorescence intensity under indicated conditions. n=3
1114 replicates, 5 averaged images per condition per replicate. **(B)** Quantification of p21
1115 nuclear fluorescence intensity under indicated conditions. n=3 replicates, 5 averaged
1116 images per condition per replicate. **(C)** Quantification of Ki67 nuclear fluorescence
1117 intensity under indicated conditions. n=3 replicates, 5 averaged images per condition
1118 per replicate. **(D)** Quantification of pRB nuclear fluorescence intensity under indicated
1119 conditions. n=3 replicates, 5 averaged images per condition per replicate. **(E)**
1120 Representative images of HAEC under static (non-flow) or Flow-E conditions with EdU
1121 incorporation and fixation at indicated times post Flow-E release. Cells stained for DAPI
1122 (white, nuclear mask) and EdU (red, S-phase), Scale bar, 50 μm. White arrow, flow
1123 direction. **(F)** Quantification of EdU+ cells under indicated conditions. n=3 replicates, 5
1124 images per condition per replicate. **(G)** Representative images of HUVEC stained with
1125 VE-cadherin (white, junction marker) and DAPI (blue, nucleus) under indicated
1126 conditions. Scale bar, 50 μm. White arrow, flow direction. **(H)** Cell axis ratio
1127 quantification under indicated conditions. n=3 replicates, 5 images per condition per
1128 replicate. **(I)** % HUVEC under Flow-E release with p27-/EdU-, p27+/EdU-, and p27-
1129 /EdU+ incorporation. **(J)** % HUVEC under high density release with p27-/EdU-,
1130 p27+/EdU-, and p27-/EdU+ incorporation. Statistics, one-way ANOVA with Tukey's
1131 multiple comparisons test (A-D, F, H) and X^2 test (I-J).
1132

1133 **Supplemental Figure 6. Nuclear fluorescence intensity of markers and changes**
1134 **with *HES1* or *ID3* depletion.**
1135 **(A)** RT-qPCR for *HES1* expression under indicated conditions. n=3 replicates. **(B)** RT-
1136 qPCR for *ID3* expression under indicated conditions, n=3 replicates. **(C)** Quantification
1137 of p27 nuclear fluorescence intensity with indicated siRNA treatments and conditions.
1138 n=3 replicates, 5 averaged images per condition per replicate. **D)** Representative
1139 images of HAEC under indicated conditions and with indicated siRNA treatment. Cells
1140 stained for p27 (green) and DAPI (white, nuclear mask). Scale bar, 50 μm. White arrow,
1141 flow direction. **(E)** Quantification of p27+ cells under indicated conditions and
1142 treatments. n=3 replicates, 5 images per condition per replicate. **(F)** Representative
1143 images of HUVEC under indicated conditions and siRNA treatments. Cells were labeled
1144 with EdU (red, S-phase) and stained for DAPI (white, nuclear mask). Scale bar, 50 μm.
1145 White arrow, flow direction. **(G)** Quantification of EdU+ cells with indicated conditions.
1146 n=3 replicates, 5 images per condition per replicate. **(H)** Quantification of pRB nuclear
1147 fluorescence intensity under indicated siRNA treatments and conditions. n=3 replicates,
1148 5 averaged images per condition per replicate. **(I)** Quantification of pRB nuclear
1149 fluorescence intensity under indicated siRNA treatments and conditions. n=3 replicates,
1150 5 averaged images per condition per replicate. Statistics, student's two tailed t-test (A-
1151 B) and one-way ANOVA with Tukey's multiple comparisons test (C, E, G-I).
1152

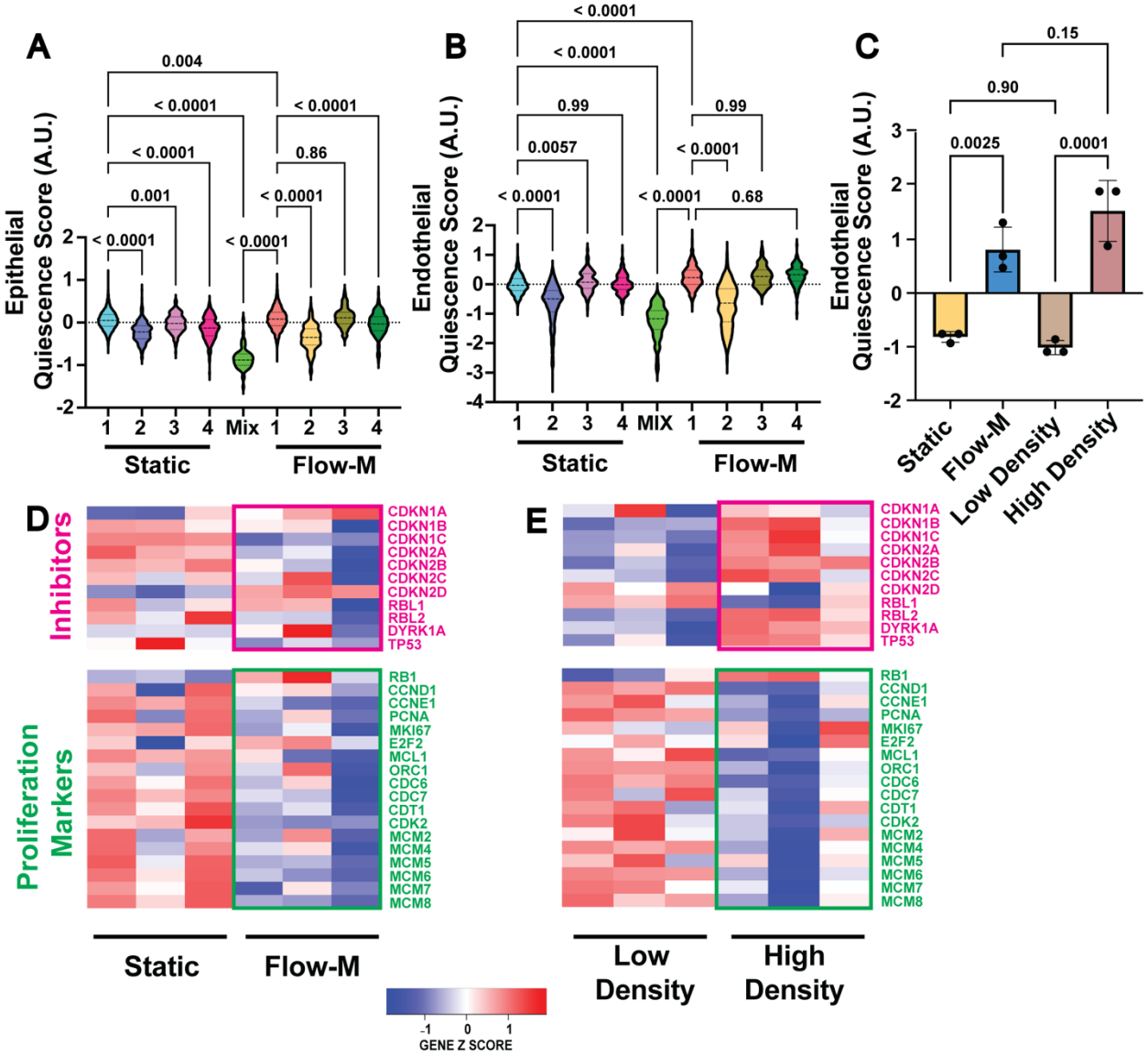

Figure 1. Laminar flow-mediated quiescence is transcriptionally distinct. **(A)** Quantification of epithelial quiescence score in HUVEC scRNA dataset by cluster (previously defined[8]). Flow-M, flow maintenance (laminar flow (15d/cm^2/72h)). Static cells were visually checked for subconfluence and collected 48h post-seeding. **(B)** Quantification of endothelial quiescence score in HUVEC scRNA dataset by cluster. **(C)** Endothelial quiescence score on bulk RNA seq data of HUVEC exposed to indicated stimuli, n= 3 replicates. **(D-E)** Heatmaps showing relative expression of cell cycle proliferation markers (green font) and inhibitors (red font) plotted using bulk RNAseq data of HUVEC under indicated conditions, n=3 replicates. Statistics, one-way ANOVA with Tukey's multiple comparison test.

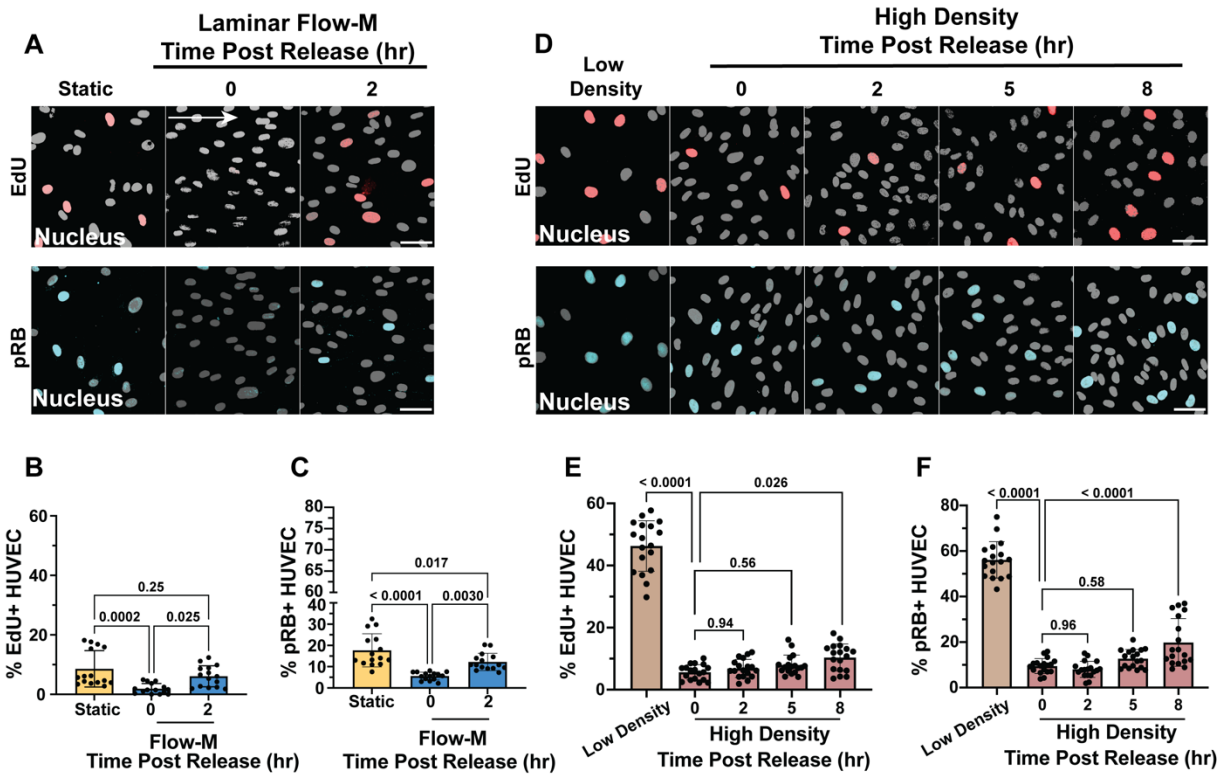

Figure 2. Endothelial cell flow maintenance quiescence stimulus leads to shallow quiescence depth.
(A) Representative images of HUVEC under static (non-flow) or Flow-M (flow maintenance) conditions with EdU incorporation and fixation at indicated times post Flow-M release. Cultures stained for DAPI (white, nuclear mask) and EdU (red, S-phase) or pRB (blue, interphase). Scale bar, 50 µm. White arrow, flow direction. **(B)** Quantification of percent EdU+ cells with indicated conditions. n=3 replicates, 5 images per condition per replicate. **(C)** Quantification of percent pRB+ cells with indicated conditions. n=3 replicates, 5 images per condition per replicate. **(D)** Representative images of HUVEC under indicated density conditions with EdU incorporation and fixation at indicated times post high-density release. Cultures stained for DAPI (white, nuclear mask) and EdU (red, S-phase) or pRB (blue, interphase). Scale bar, 50 µm. **(E)** Quantification of percent EdU+ cells with indicated conditions. n=3 replicates, 6 images per condition per replicate. **(F)** Quantification of percent pRB+ cells with indicated conditions. n=3 replicates, 6 images per condition per replicate. Statistics, one-way ANOVA with Tukey's multiple comparisons test.

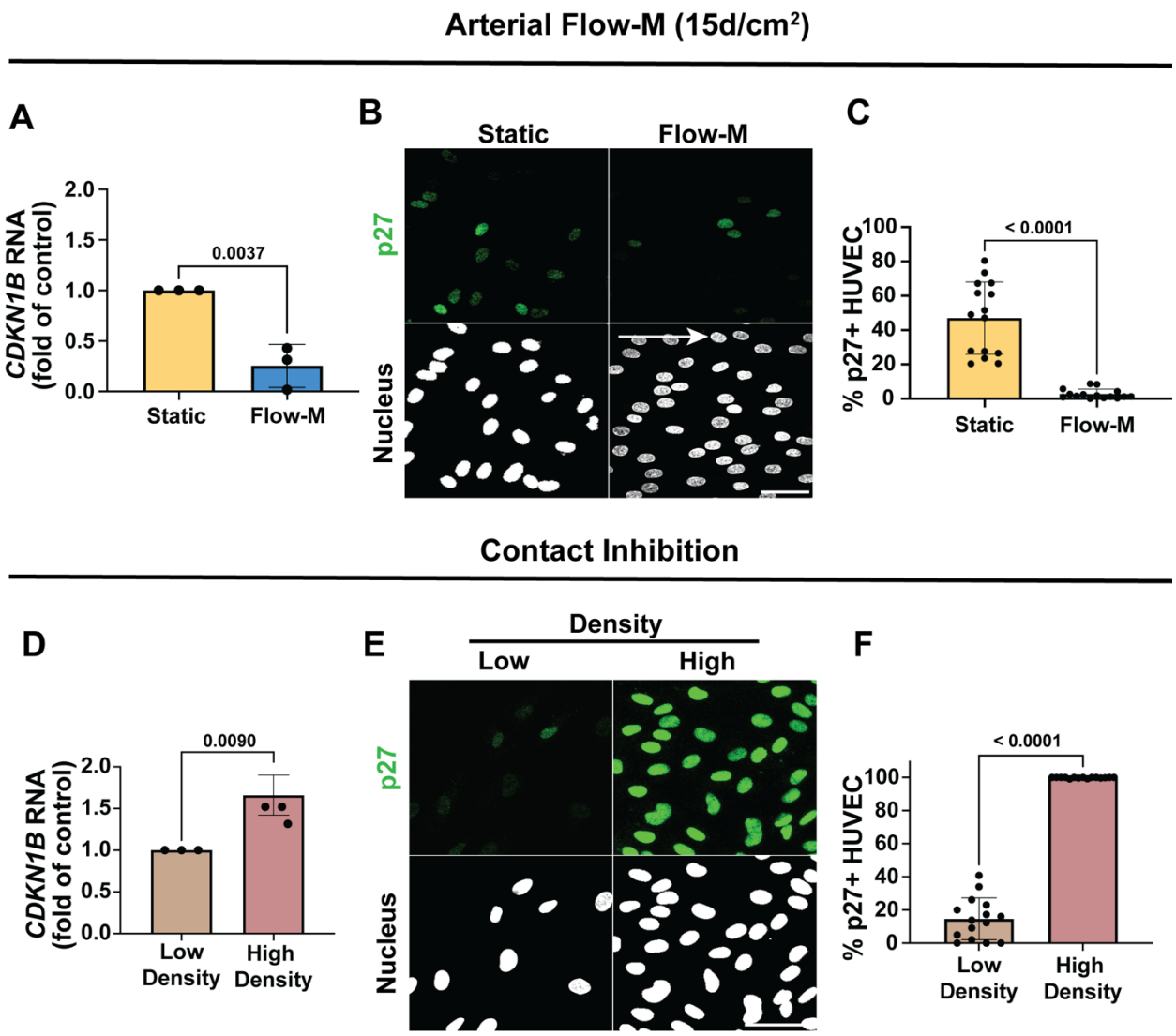

Figure 3. Cell cycle inhibitor p27 expression levels vary with endothelial quiescence stimulus.
(A) RT-qPCR for *CDKN1B* levels under indicated conditions. n=3 replicates. **(B)** Representative images of HUVEC under indicated conditions stained for p27 (green) and DAPI (white, nuclear mask). Scale bar, 50 µm. White arrow, flow direction. **(C)** Quantification of HUVEC p27+ cells under indicated conditions. n=3 replicates, 5 images per condition per replicate. **(D)** RT-qPCR for *CDKN1B* levels under indicated conditions. n=3 replicates. **(E)** Representative images of HUVEC under indicated conditions stained for p27 (green) and DAPI (white, nuclear mask). Scale bar, 50 µm. **(F)** Quantification of HUVEC p27+ cells under indicated conditions. n=3 replicates, 5 images per condition per replicate. Statistics, student's two-tailed *t*-test.

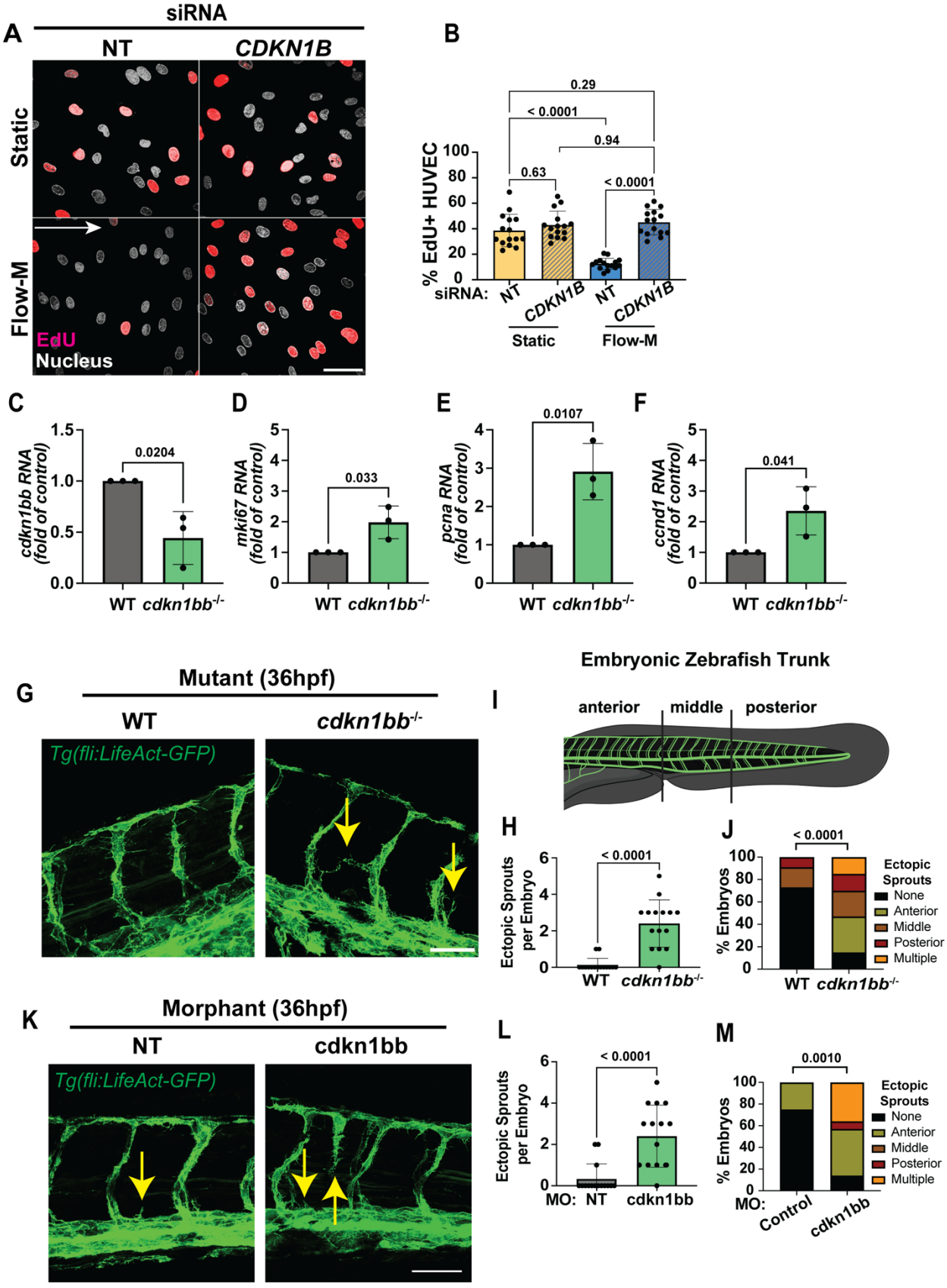
A
siRNA
NT
CDKN1B
Static
Flow-M
EdU
Nucleus
B
% EdU+ HUVEC
siRNA: NT CDKN1B NT CDKN1B
Static
Flow-M
0.29
< 0.0001
0.94
0.63
< 0.0001
C
cdkn1bb RNA (fold of control)
0.0204
WT cdkn1bb-/-
D
mki67 RNA (fold of control)
0.033
E
pcna RNA (fold of control)
0.0107
F
ccnd1 RNA (fold of control)
0.041
G
Mutant (36hpf)
WT
cdkn1bb-/-
Tg(fli:LifeAct-GFP)
Embryonic Zebrafish Trunk
I
anterior
middle
posterior
H
Ectopic Sprouts per Embryo
< 0.0001
J
% Embryos
Ectopic Sprouts
None
Anterior
Middle
Posterior
Multiple
K
Morphant (36hpf)
NT
cdkn1bb
L
MO: NT cdkn1bb
M
MO: Control cdkn1bb
0.0010

1319 **Figure 4. p27 establishes quiescence in endothelial cells and regulates cell cycle**
1320 **and vascular expansion *in vivo*.**
1321 **(A)** Representative images of HUVEC with indicated siRNA treatments and conditions.
1322 after EdU incorporation (red, S-phase) and staining with DAPI (white, nuclear mask).
1323 Scale bar, 50 µm. White arrow, flow direction. **(B)** Quantification of EdU+ cells with
1324 indicated conditions. n=3 replicates, 5 images per condition per replicate. **(C-F)** RT-
1325 qPCR of FACs sorted 24 hpf zebrafish endothelial cells from *Tg(fli:LifeAct-GFP)* (green,
1326 endothelial cell marker) embryos of indicated genotypes for *cdkn1bb* **(C)***, mki67* **(D)***,*
1327 *pcna* **(E)***,* and *ccnd1* **(F)** levels. n=3 replicates. **(G)** Representative images of 36hpf
1328 *Tg(fli:LifeAct-GFP)* (green, endothelial cell marker) embryos that were also WT or
1329 *cdkn1bb*$^{-/-}$. Yellow arrows, ectopic sprouts. Scale bar, 50 µm. **(H)** Quantification of
1330 ectopic sprouts per embryo. n=3 replicates, 5 images per condition per replicate. **(I)**
1331 Diagram defining regions for ectopic sprout quantification in embryonic zebrafish. **(J)**
1332 Quantification of % ectopic sprouts in *Tg(fli:LifeAct-GFP)* (green, endothelial cell
1333 marker) embryos and of indicated genotypes per region. n=3 replicates, 5 images per
1334 condition per replicate. **(K)** Representative images of 36hpf *Tg(fli:LifeAct-GFP)* embryos
1335 injected with control (NT) or cdkn1bb MO at the one-cell stage. Yellow arrows, ectopic
1336 sprouts. Scale bar, 50 µm. **(L)** Quantification of ectopic sprouts per embryo. n=3
1337 replicates, 5 images per condition per replicate. **(M)** Quantification of % ectopic sprouts
1338 in *Tg(fli:LifeAct-GFP)* (green, endothelial cell marker) and with indicated MO injection
1339 per region. n=3 replicates, 5 images per condition per replicate. Statistics, student's two-
1340 tailed *t*-test (C-F, H, L), one-way ANOVA with Tukey's multiple comparisons test (B),
1341 and C^2 test (J, M).
1342

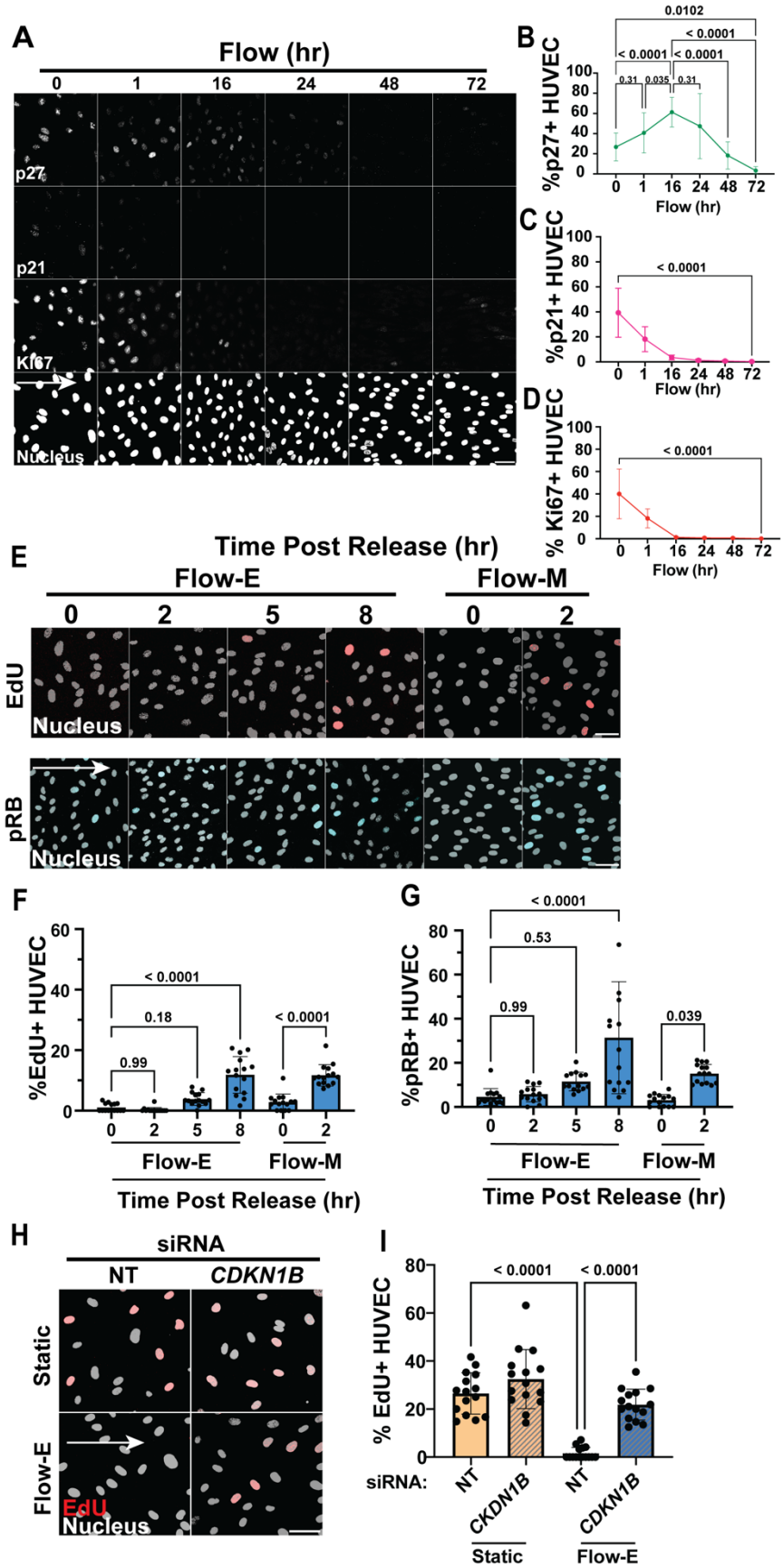
A
Flow (hr)
0 1 16 24 48 72
p27
p21
Ki67
Nucleus
B
%p27+ HUVEC
Flow (hr)
0.0102
< 0.0001
< 0.0001
< 0.0001
0.31
0.035
0.31
C
%p21+ HUVEC
< 0.0001
D
% Ki67+ HUVEC
< 0.0001
E
Time Post Release (hr)
Flow-E
Flow-M
0 2 5 8 0 2
EdU
pRB
Nucleus
F
%EdU+ HUVEC
< 0.0001
0.18
0.99
< 0.0001
Flow-E
Flow-M
Time Post Release (hr)
G
%pRB+ HUVEC
< 0.0001
0.53
0.99
0.039
Flow-E
Flow-M
Time Post Release (hr)
H
siRNA
NT
CDKN1B
Static
Flow-E
EdU
Nucleus
I
% EdU+ HUVEC
< 0.0001
< 0.0001
siRNA:
NT
CKDN1B
NT
CDKN1B
Static
Flow-E

1387 **Figure 5. Endothelial quiescence depth varies with laminar flow exposure time**
1388 **and positively correlates with p27 expression levels.**
1389 **(A)** Representative images of HUVEC with indicated conditions and stained for p27
1390 (inhibitor), p21 (inhibitor), Ki67 (proliferation marker), and DAPI (nucleus) in white. Scale
1391 bar, 50 µm. White arrow, flow direction. **(B-D)** Quantification of percent p27+ (**B**), p21+
1392 cells (**C**), or Ki67+ cells (**D**). n=3 replicates, 5 images per condition per replicate. **(E)**
1393 Representative images of HUVEC under indicted conditions and after EdU incorporation
1394 (red, S-phase) and stained for pRB (blue, interphase) and with DAPI (white, nuclear
1395 mask), Flow-E, flow establishment (15d/cm^2, 16h); Flow-M, flow maintenance (15d/cm^2,
1396 72h). Scale bar, 50 µm. White arrow, flow direction. **(F)** Quantification of EdU+ cells
1397 under indicated conditions. n=3 replicates, 5 images per condition per replicate. **(G)**
1398 Quantification of pRB+ cells under indicated conditions. n=3 replicates, 5 images per
1399 condition per replicate. **(H)** Representative images of HUVEC with indicated siRNA
1400 treatments and conditions after EdU incorporation (red, S-phase) and staining with
1401 DAPI (white, nuclear mask). Scale bar, 50 µm. White arrow, flow direction. **(I)**
1402 Quantification of EdU+ cells with indicated conditions. n=3 replicates, 5 images per
1403 condition per replicate. Statistics, one-way ANOVA with Tukey's multiple comparisons
1404 test.
1405

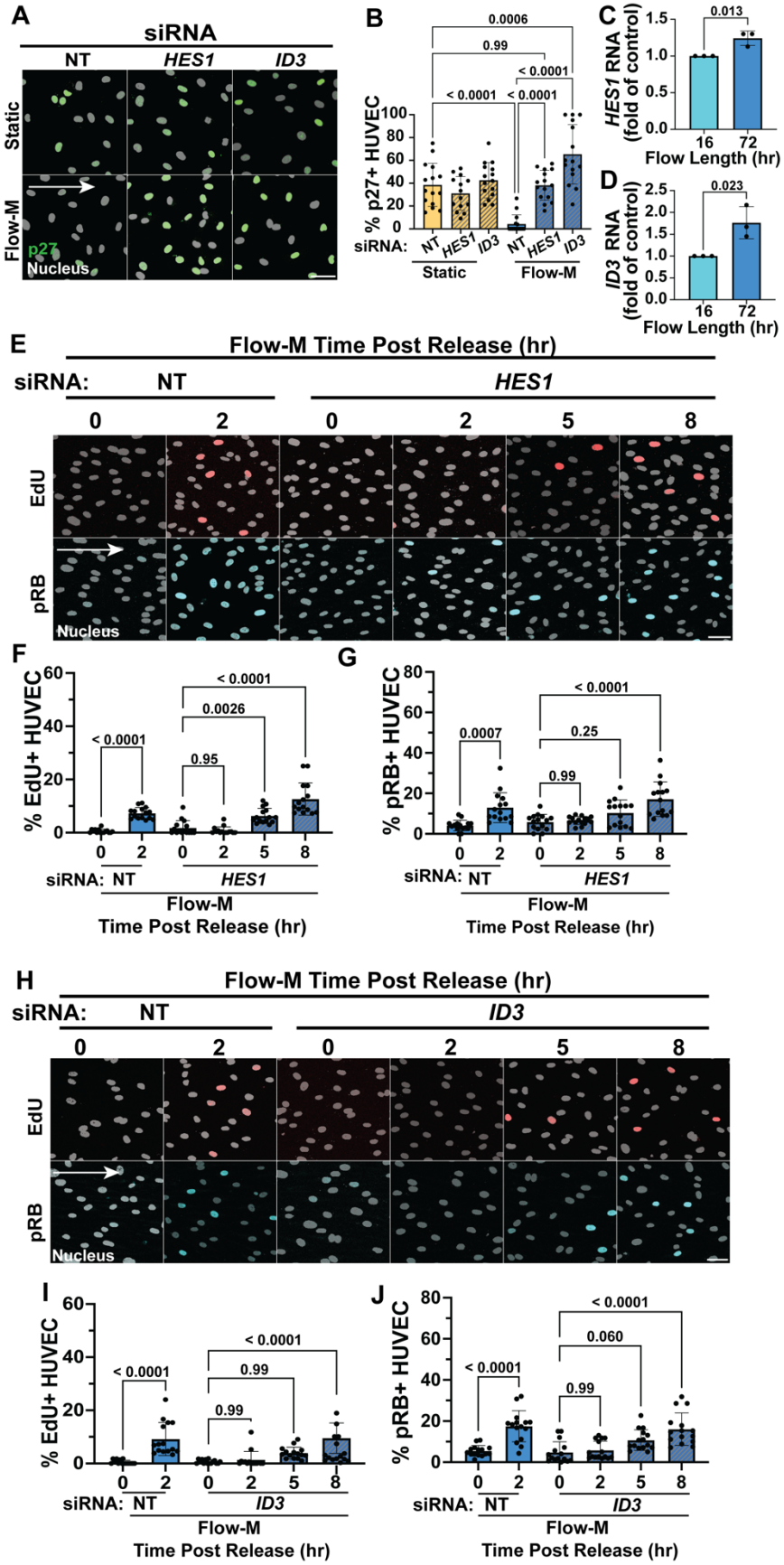
A
siRNA
NT
HES1
ID3
Static
Flow-M
p27
Nucleus
B
% p27+ HUVEC
0.0006
0.99
< 0.0001
< 0.0001
< 0.0001
siRNA: NT HES1 ID3 NT HES1 ID3
Static
Flow-M
C
HES1 RNA (fold of control)
0.013
16 72
Flow Length (hr)
D
ID3 RNA (fold of control)
0.023
16 72
Flow Length (hr)
E
Flow-M Time Post Release (hr)
siRNA: NT HES1
0 2 0 2 5 8
EdU
pRB
Nucleus
F
% EdU+ HUVEC
< 0.0001
0.0026
< 0.0001
0.95
siRNA: NT HES1
Flow-M
Time Post Release (hr)
G
% pRB+ HUVEC
0.0007
< 0.0001
0.25
0.99
siRNA: NT HES1
Flow-M
Time Post Release (hr)
H
Flow-M Time Post Release (hr)
siRNA: NT ID3
0 2 0 2 5 8
EdU
pRB
Nucleus
I
% EdU+ HUVEC
< 0.0001
< 0.0001
0.99
0.99
siRNA: NT ID3
Flow-M
Time Post Release (hr)
J
% pRB+ HUVEC
< 0.0001
< 0.0001
0.060
0.99
siRNA: NT ID3
Flow-M
Time Post Release (hr)

1450 **Figure 6. BMP and NOTCH regulated p27 repressors *HES1* and *ID3* regulate p27**
1451 **levels and flow-mediated quiescence depth.**
1452 **(A)** Representative images of HUVEC under indicated conditions and with indicated
1453 siRNA treatment. Cells stained for p27 (green) and DAPI (white, nuclear mask). Scale
1454 bar, 50 µm. White arrow, flow direction. **(B)** Quantification of p27+ cells under indicated
1455 conditions and treatments. n=3 replicates, 5 images per condition per replicate. **(C-D)**
1456 RT-qPCR for *HES1* **(C)** and *ID3* **(D)** levels under indicated conditions. n=3 replicates.
1457 **(E)** Representative images of HUVEC under indicated conditions and siRNA treatments.
1458 Cells were labeled with EdU (red, S-phase) and stained for pRB (blue, interphase) and
1459 DAPI (white, nuclear mask). Scale bar, 50 µm. White arrow, flow direction. **(F)**
1460 Quantification of EdU+ cells with indicated conditions. n=3 replicates, 5 images per
1461 condition per replicate. **(G)** Quantification of pRB+ cells with indicated conditions. n=3
1462 replicates, 5 images per condition per replicate. **(H)** Representative images of HUVEC
1463 under indicated conditions and siRNA treatments. Cells were labeled with EdU (red, S-
1464 phase) and stained for pRB (blue, interphase) and DAPI (white, nuclear mask). Scale
1465 bar, 50 µm. White arrow, flow direction. **(I)** Quantification of EdU+ cells under indicated
1466 conditions. n=3 replicates, 5 images per condition per replicate. **(J)** Quantification of
1467 pRB+ cells under indicated conditions. n=3 replicates, 5 images per condition per
1468 replicate. Statistics, student's two-tailed *t*-test (C-D) and one-way ANOVA with Tukey's
1469 multiple comparisons test (B, F-G, I-J).
1470

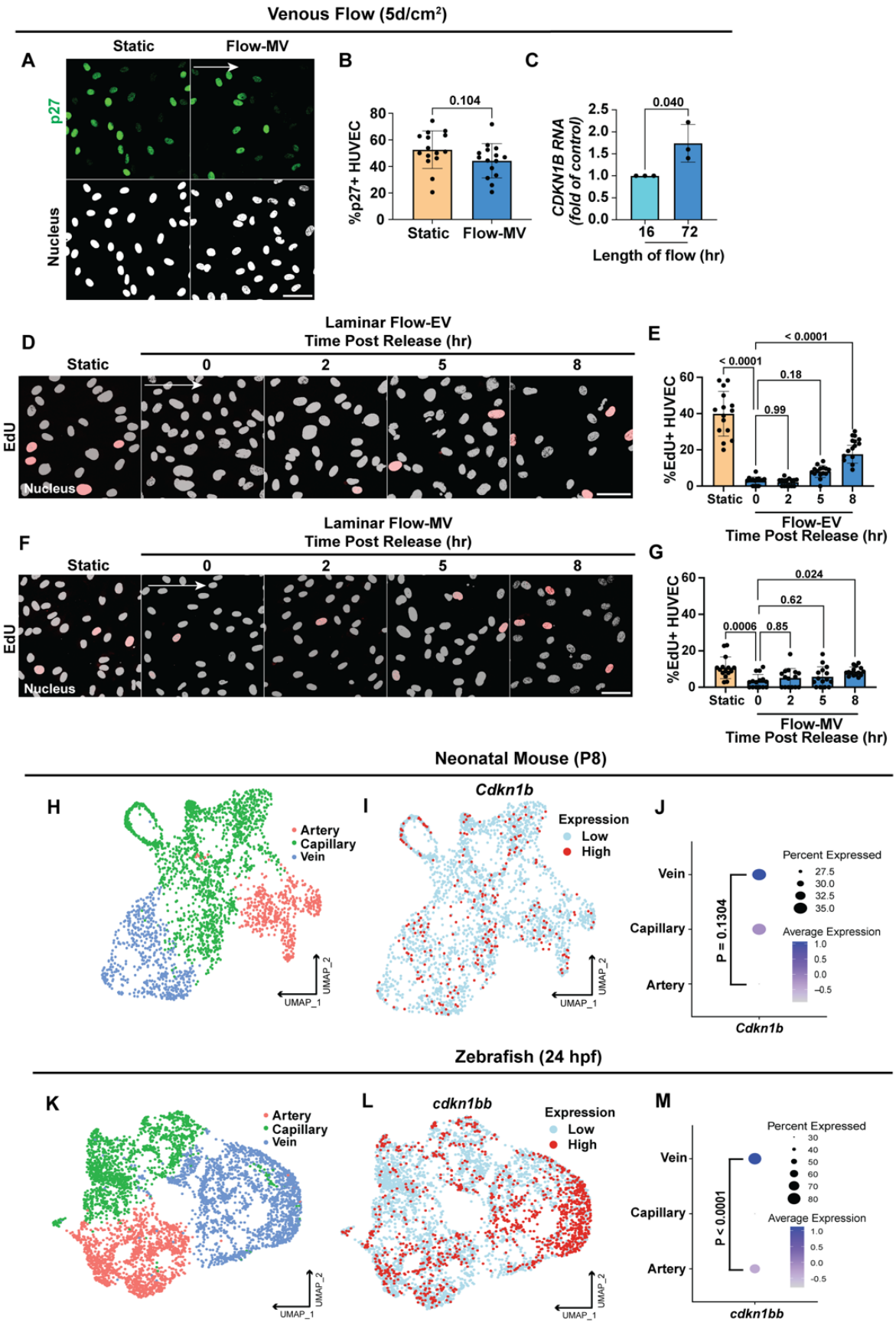
Venous Flow (5d/cm²)
A
Static
Flow-MV
p27
Nucleus
B
%p27+ HUVEC
0.104
Static
Flow-MV
C
CDKN1B RNA (fold of control)
0.040
16
72
Length of flow (hr)
Laminar Flow-EV
Time Post Release (hr)
D
Static
0
2
5
8
EdU
Nucleus
E
%EdU+ HUVEC
< 0.0001
< 0.0001
0.18
0.99
Static
Flow-EV
Time Post Release (hr)
Laminar Flow-MV
Time Post Release (hr)
F
G
0.024
0.62
0.0006
0.85
Flow-MV
Time Post Release (hr)
Neonatal Mouse (P8)
H
Artery
Capillary
Vein
UMAP_1
UMAP_2
I
Cdkn1b
Expression
Low
High
J
Percent Expressed
Average Expression
P = 0.1304
Vein
Capillary
Artery
Cdkn1b
Zebrafish (24 hpf)
K
L
cdkn1bb
M
P < 0.0001
cdkn1bb

1515 **Figure 7. Endothelial cells establish and maintain deep quiescence under venous**
1516 **flow and express elevated p27 levels *in vivo*.**
1517 **(A)** Representative images of HUVEC under indicated conditions (Flow-MV (5d/cm^2,
1518 72h)) stained for p27 (green) and DAPI (white, nuclear mask). Scale bar, 50 µm. White
1519 arrow, flow direction. **(B)** Quantification of HUVEC p27+ cells under indicated
1520 conditions, n=3 replicates, 5 images per condition per replicate. **(C)** RT-qPCR for
1521 *CDKN1B* levels in indicated conditions. n=3 replicates. **(D)** Representative images of
1522 HUVEC under static (non-flow) or Flow-EV (5d/cm^2, 16h) conditions with EdU
1523 incorporation and fixation at indicated times post Flow-EV release. Cells stained for
1524 DAPI (white, nuclear mask) and EdU (red, S-phase), Scale bar, 50 µm. White arrow,
1525 flow direction. **(E)** Quantification of EdU+ cells with indicated conditions. n=3 replicates,
1526 5 images per condition per replicate. **(F)** Representative images of HUVEC under static
1527 (non-flow) or Flow-MV conditions (5d/cm^2, 72h) with EdU incorporation and fixation at
1528 indicated times post Flow-MV release. Cells stained for DAPI (white, nuclear mask) and
1529 EdU (red, S-phase), Scale bar, 50 µm. White arrow, flow direction. **(G)** Quantification of
1530 EdU+ cells with indicated conditions. n=3 replicates, 5 images per condition per
1531 replicate. **(H)** UMAP grouping of artery, vein, and capillary endothelial cell clusters
1532 enriched from neonatal mouse ear skin. **(I)** UMAP overlaid with *Cdkn1b (p27)*
1533 expression. **(J)** Dot plot of *Cdkn1b* expression by endothelial sub-type. **(K)** UMAP
1534 grouping of endothelial artery, vein, and capillary clusters reanalyzed from 24hpf
1535 embryonic zebrafish. **(L)** UMAP overlaid with *cdkn1bb (p27)* expression. **(M)** Dot plot of
1536 *Cdkn1b* expression by endothelial sub-type. Statistics, student's two-tailed *t*-test (B-C,
1537 J-M) and one-way ANOVA with Tukey's multiple comparisons test (E, G).
1538

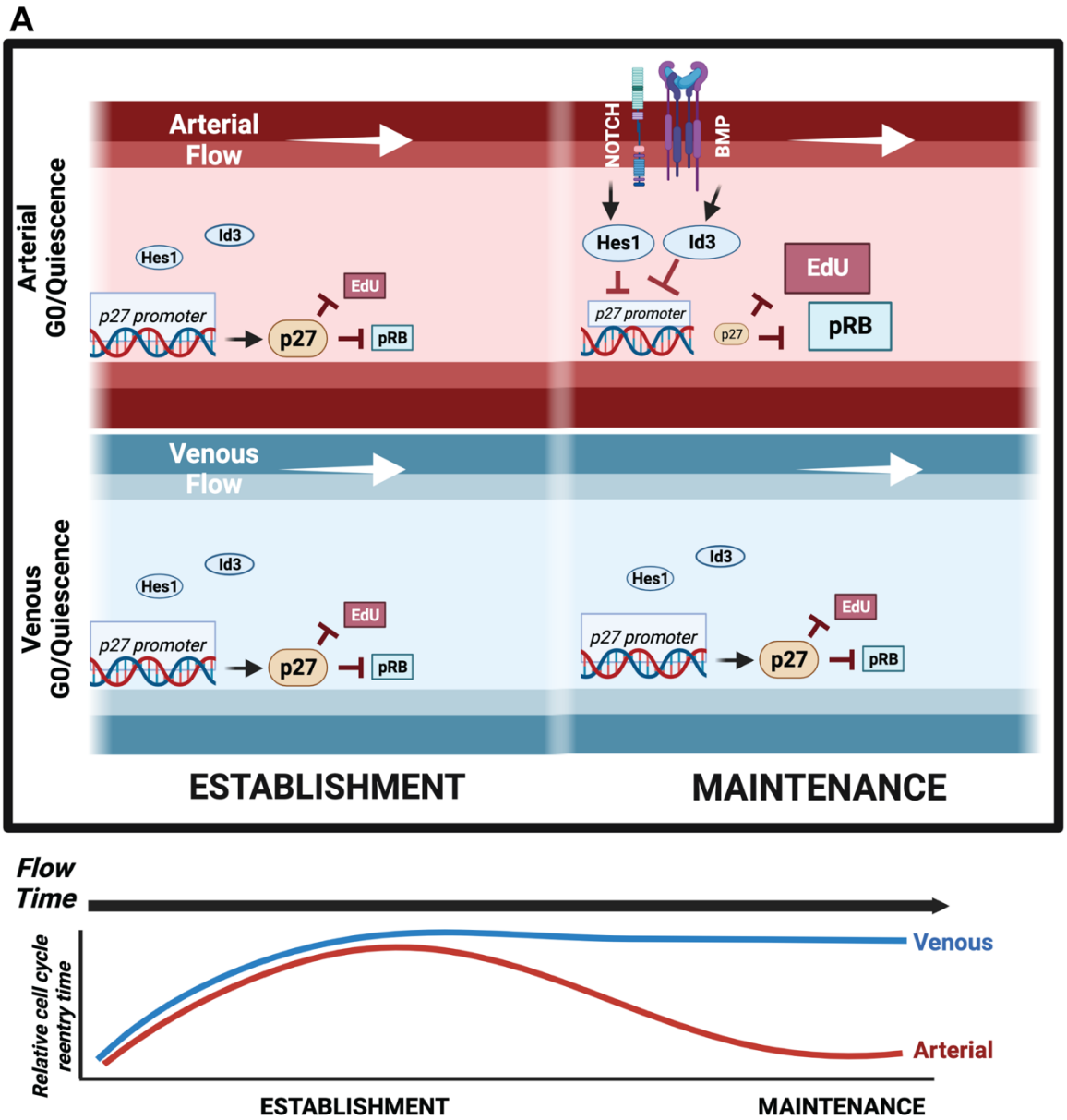

Figure 8. ***Model of endothelial cell flow-mediated quiescence depth.*** Proposed model for dynamic regulation of endothelial cell flow-mediated quiescence depth with flow exposure time and magnitude. In the first 16h (Flow-E, arterial flow establishment) of laminar flow, a deep quiescence is established accompanied by high levels of cell cycle inhibitor p27, independent of flow magnitude. With time under arterial flow (Flow-M, flow maintenance), *HES1* and *ID3* transcription factors are upregulated downstream of flow-mediated Notch and BMP signaling, and they repress p27 transcription leading to a shallow quiescence depth. Deep quiescence and high p27 levels characterize venous flow establishment at 16h (Flow-EV, venous flow establishment), and this deep quiescence perdures with time under venous flow (Flow-MV).